Unitary, relativistic resonance model for πN scattering

Franz Gross
College of William and Mary, Williamsburg, Virginia 23185
and Continuous Electron Beam Accelerator Facility, 12000 Jefferson Ave., Newport News, Virginia 23606

Yohanes Surya
College of William and Mary, Williamsburg, Virginia 23185
(Received 14 September 1992)

Pion nucleon scattering up to 600 MeV laboratory kinetic energy is described by a manifestly covariant wave equation in which the pion is restricted to its mass shell. The kernel of the equation includes nucleon (N), Roper (N^*), delta (Δ), and D_{13} poles, with their corresponding crossed pole terms approximated by contact interactions, and contact σ- and ρ-like exchange terms. The πNN vertex is treated as a mixture of γ^5 and $\gamma^\mu\gamma^5$ coupling, with a mixing parameter λ chosen so that the dressed nucleon pole will be unshifted by the interaction. Chiral symmetry is maintained at threshold. The resonance contributions are fully unitarized by the equation, with their widths determined by the dynamics included in the model. The Δ and D_{13} are treated as a pure spin $\frac{3}{2}$ particles, with no spin $\frac{1}{2}$ amplitude in the S channel. The complete development of this model, which gives a very good fit to all the data up to 600 MeV, is presented.

PACS number(s): 21.30.+y, 13.75.Gx, 24.10.Jv

I. OVERVIEW, RESULTS, AND CONCLUSION

A. Introduction

Pion nucleon scattering has been studied thoroughly for many years. One of the best known early models, which treated the nucleon nonrelativistically, was introduced by Chew and Low in 1956 [1]. This model described low energy P-wave scattering very well, but had to be modified in order to describe S-wave scattering [2]. Among later efforts is the work based in current algebra [3, 4] and Lagrangian models based on chiral symmetry [5–7]. More recently, Banerjee and Cammarata [8] have extended the Chew-Low model to include nucleon recoil and antinucleon contributions, and Pearce and Jennings [9], using a Lagrangian model and a relativistic wave equation, have extended the analysis up to pion laboratory kinetic energies of 400 MeV.

However, with the construction of powerful new facilities such as the Continuous Electron Beam Accelerator Facility (CEBAF), it is necessary to have a good description of πN scattering which extends up to higher energies. Such a description must be covariant, and include not only the nucleon (N) and delta (Δ) resonances, but also the Roper (N^*), which plays a prominent role in the P_{11} channel at energies above 400 MeV, and the $D_{13}(1520)$, which makes a significant contribution to the total isospin $\frac{1}{2}$ cross section near 600 MeV.

In this paper we present a simple, covariant, and unitary model of πN scattering which works well up to 600 MeV. These are essential features of a πN model which is to be used as a reliable input to other model calculations, such as the calculation of NN scattering up to nucleon laboratory kinetic energies of 1 GeV, where the excitations of pion degrees of freedom become important. It is with such applications in mind that this model has been developed.

In this work the πN scattering amplitude is obtained as a solution of a relativistic wave equation in which the pion is restricted to its mass shell in all intermediate states. The rationale for this approach is described in Sec. II A. In order to describe the πN resonances at T_π laboratory ~ 187, ~ 485, and ~ 611 MeV, the kernel (sometimes referred to as Born or "driving" terms) of the relativistic integral equation includes undressed Δ, N^*, and D_{13} poles in addition to the undressed nucleon pole. We make no attempt to explain these bare, undressed states within the model; they are presumably explained by quark models in the same way that the nucleon state is explained. The kernel also includes contributions derived from crossed N, Δ, N^*, and D_{13} diagrams, and from σ- and ρ-like exchange terms. To simplify the equation, and obtain analytic solutions, these latter terms are approximated by a contact interaction, as described in Sec. III. The approximations used to obtain the contact terms give zero for the crossed Δ and D_{13} poles. All of these driving terms are shown diagrammatically in Fig. 1. The solution which emerges from the integral equation automatically satisfies unitary, and dresses the resonance poles by shifting their masses and giving them a width, and hence our model complements quark models by adding the pion interactions sometimes omitted from such models. For reasons which we will discuss in some detail below, we adjust the parameters of the model so that the dressed nucleon pole is *not shifted by the interaction.*

For the πNN coupling we use a superposition of both pseudoscalar (γ^5) and pseudovector ($\gamma^5\gamma^\mu$) cou-

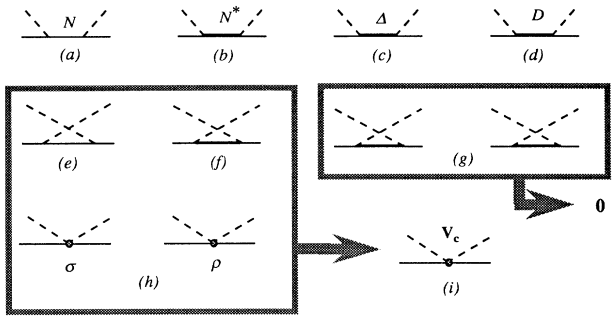

FIG. 1. Born terms which make up the kernel of the integral equation used in this paper. The diagrams in box (h) are eventually approximated by a contact term, shown in (i).

pling, with a mixing parameter λ defined so that the coupling is independent of λ when *both the incoming and outgoing nucleon are on shell.* This mixed coupling was used succesfully in one boson exchange models of NN scattering by Gross, Van Orden, and Holinde [10, 11], who found that a small admixture (about 25%) of γ^5 coupling made it possible to fit the data with a minimum of exchanged mesons. One of the purposes of this study was to see if this mixed coupling had any justification within the framework of πN scattering.

The Δ and D_{13} are treated as pure spin 3/2 particles, using a spin 3/2 projection operator proposed by Behrends and Fronsdal [12], and recently discussed by Williams [13], and their widths emerge automatically as a dynamical consequence of unitarity. We also introduce a new form for the $\pi N\Delta$ and πND_{13} vertices. The combination of the spin 3/2 projection operator and this new vertex not only makes the calculation simpler but also eliminates all spin 1/2 amplitudes. Some authors [14] have argued that these virtual spin 1/2 amplitudes, which must be present if the spin 3/2 propagator is to have an inverse, are an important feature of the physics. We obtain a very successful fit without them. The D_{13} is inelastic, and in this model we allow for this by coupling the D_{13} to the $\pi\Delta$ channel, which gives an excellent description of the data.

The role of the Roper, especially at low energies, has been questioned for many years. Many authors [9, 15, 16] do not include the Roper, even in their description of the P_{11} channel. They argue that a cancellation between the direct and crossed N pole terms can explain the unique behavior of P_{11} partial wave, which is negative at low energy and changes sign at T_π laboratory $\sim$ 150 MeV. Oset, Taki, and Weise [17] argue that the change of sign is due to the cancellation of the N and Roper pole terms, but they treated the Roper only at the tree level. In this paper we include $N^* \leftrightarrow N^*$ and $N^* \leftrightarrow N$ mixing to all orders, our result is unitary, and the Roper width emerges as a natural consequence of the dynamics. We also include the inelastic coupling of the Roper to the $\pi\Delta$ channel, which is its dominant inelastic decay mode [18].

We conclude this brief introduction by summarizing the novel features of this model, which to our knowledge have not been studied before in the context of πN scattering: (i) the scattering amplitude is the solution of a relativistic wave equation in which the pion is restricted to its mass shell in all intermediate states; (ii) the πNN coupling is taken to be a superposition of both pseudoscalar (γ^5) and pseudovector ($\gamma^5\gamma^\mu$) coupling; (iii) the nucleon self-energy is constrained to be *zero* at the nucleon pole, so that the nucleon mass remains unshifted by the interactions; (iv) the Δ and D_{13} are pure spin $\frac{3}{2}$ particles, with widths which develop naturally from the unitarity of the solution; and (v) contributions from the Roper (N^*) and $N^* \leftrightarrow N$ transition amplitudes are iterated to all orders, giving a consistent description of the Roper and its width.

These new features are discussed in the following sections of this section, which also includes a presentation of the numerical results, discussion and conclusion. Section II presents the relativistic formalism including the partial wave expansion and a discussion of unitarity. The construction and the development of the relativistic kernel are presented in Sec. III where the treatment of the Roper (N^*), Δ, and D_{13} is described in some detail. The appendixes discuss some technical points.

B. Restricting the pion to its mass shell

One way to ensure that a scattering amplitude is both covariant and unitary is to obtain it as a solution of a covariant integral equation. Solving the equation automatically iterates its kernel to all orders, and gives a unitary amplitude.

The Bethe-Salpeter (BS) equation is one possible starting point for a relativistic description of πN scattering. If the πN scattering matrix is $\mathbf{M}$, then the BS equation is

$$\mathbf{M}(p',p;P) = \mathbf{V}(p',p;P) + i\int \frac{d^4k}{(2\pi)^4}\mathbf{V}(p',k;P)\,G_{\rm BS}(k,P)\,\mathbf{M}(k,p;P), \tag{1.1}$$

where $\mathbf{V}(p',p;P)$ is the relativistic kernel, $G_{\rm BS}(k,P)$ is the free relativistic two particle Green's function (two-body propagator), and p, p', k, and P are the four-momenta of the incoming nucleon, outgoing nucleon, intermediate pion, and the total four-momentum of the system, as shown in Fig. 2. The integration is over all four components of the pion four-momentum, and for this reason the equation is described an a "four-dimensional" equation. The *exact* πN scattering amplitude can be obtained from the BS equation only if its kernel includes the sum of *all connected two particle irreducible diagrams.* There are infinite number of these, and no known way to sum them, so that the kernel must be approximated.

One approximation is to introduce a separable interaction. In Refs. [19, 20] this approach was used to parametrize the S- and P-wave phase shifts, with a different set of parameters for each phase shift. This worked well, but the parameters have no physical interpretation,

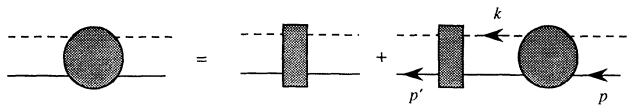

FIG. 2. Diagrammatic representation of the integral equation.

and it is difficult to relate them to masses and coupling constants.

Since the kernel must be approximated (by using a few diagrams that we believe to be especially important physically), there is not necessarily any reason to retain the full four-dimensional BS equation. There are several *covariant three-dimensional* equations [21] which can be used, and the choice depends on the physics and on the approximations being made. Recently Pearce and Jennings [9] used what they refer to as a *smooth* propagator [22] to describe πN scattering. They replace the two-body propagator of the BS equation,

$$G(k,P) = \frac{m + \not{P} - \not{k}}{(\mu^2 - k^2 - i\epsilon)[m^2 - (P-k)^2 - i\epsilon]} \tag{1.2}$$

by the propagator [22]

$$G_{sm}(\mathbf{k},P) = 2\pi \frac{\delta(\omega(W) - k_0)}{2W} \left(\frac{m + \gamma^0 E(W) + \gamma \cdot \mathbf{k}}{m^2 + \mathbf{k}^2 - E^2(W) - i\epsilon} \right), \tag{1.3}$$

where μ and m are the mass of pion and the nucleon, W is the total energy in the c.m. system, and $E(W)$ and $\omega(W)$ are the energies of the nucleon and pion when both are on shell. They derived this propagator by letting the mass of the nucleon become infinitely heavy and eliminating the short range structure from their relativistic kernel. They obtained a pretty good fit to the phase shifts up to 400 MeV.

Our approach follows from the examination of the singularities of a typical Feynman diagram which the equation will iterate, and study of these diagrams is carried out in detail in Sec. II A. We are led to conclude that the most accurate method of summing the diagrams is to put the pion on its mass shell. Since the pion is the light particle, and previous studies of scattering in which a light meson is exchanged between two heavy particles of masses $m_1 \geq m_2$ led to the conclusion that the heaviest particle (m_1) should be on shell [23, 24], the new result seems surprising at first glance, and we also explain in Sec. II A why a different conclusion is reached for the πN system.

The propagator we obtain can be written

$$G_\pi(\mathbf{k},P) = 2\pi \frac{\delta(\omega_k - k_0)}{2\omega_k} \left(\frac{m + \gamma^0(W - \omega_k) + \gamma \cdot \mathbf{k}}{E_k^2 - (W - \omega_k)^2 - i\epsilon} \right), \tag{1.4}$$

where $\omega_k = \sqrt{\mu^2 + \mathbf{k}^2}$ is the on shell energy of the pion. Not only is this propagator efficient in summing the relevant Feynman diagrams, but it also suggests some nice approximations for the relativistic kernel, as will be discussed in Sec. III.

To ensure convergence of the integral equation, we multiply all of the driving terms by form factors. Since the pions are on shell, the form factors will depend only on the virtual mass (squared) of the off-shell incoming and outgoing baryons (the N, Δ, and the N^*; no form factor is needed for the D_{13}). For example, we attach a universal function $f(p^2)$ to each off-shell nucleon entering or leaving any vertex, and so the form factor for the πNN vertex automatically assumes a factorized form $f(p^2)\,f(p'^2)$, where p and p' are the four-momenta of the incoming and outgoing nucleon, respectively. For clarity, we will defer all further discussion of the details of the definition of the form factors and the construction of the kernels to Sec. III.

C. πNN coupling

It is well known that in a model in which pions interact with nucleons which are on shell, the pseudoscalar and pseudovector πNN coupling give the same results [25]. When the nucleon is off shell this is no longer true, and the results may depend on which coupling is used. In some early perturbative calculations based on lowest order Feynman diagrams, γ^5 coupling was used because this coupling is renormalizable [26]. However, the use of γ^5 coupling for the nucleon Born terms gives an incorrect result for a_+, the πN isospin-even scattering length. This failure is associated with the fact that γ^5 coupling violates chiral symmetry unless it is accompanied by a σ exchange term with precisely the correct strength, as described (for example) by the linear σ model introduced by Gell-Mann and Levy [27] in 1960. The Born terms in this model include the exchange of a σ particle with precisely the correct strength to give good predictions in the soft pion limit. This model was further improved by Weinberg [5] and others [28], who eliminated the σ and developed nonlinear chiral Lagrangians. Models based on these Lagrangians give a good description of πN scattering in the soft pion limit without explicit reference to a σ particle. One form of these effective Lagrangians replaces the pseudoscalar coupling and effective σ term with a pseudovector coupling and a ρ term. Since then, some people have preferred to use pseudovector coupling to describe πN scattering [6, 9].

However, if one is careful to include the correct sigma term (which need not be a real σ exchange, but could be a σ-like $\pi\pi NN$ contact term), then it is still possible to use γ^5 coupling. Furthermore, one can show that a coupling consisting of a mixture of pseudoscalar and pseudovector, with a corresponding mixture of σ-like and ρ-like contact terms, is completely equivalent *in the Born approximation* to either γ^5 or $\gamma^5\gamma^\mu$ coupling alone. Specifically, consider a mixed πNN coupling of the form

$$g\,\tau_i \left[\lambda\gamma^5 - (1-\lambda)\frac{(\not{p} - \not{p}')}{2m}\gamma^5 \right], \tag{1.5}$$

where p and p' are the four-momenta of the initial and final nucleon, respectively, i is the isospin index for the pion, and λ is the mixing parameter. (The vertex also includes nucleon form factors, omitted here for simplicity; see Sec. III.) In this form, we can easily see that when λ is zero the coupling is purely pseudovector and when it is unity the coupling is pure pseudoscalar, and also that the coupling will be independent of λ if both initial and final nucleons are on shell. Next, consider a $\pi\pi NN$ contact term of the form

$$-C\frac{g^2}{m}\left[\lambda^2\,\delta_{ij}+(1-\lambda)^2\,[\tau_j,\tau_i]\,\frac{\not{Q}}{4m}\right], \qquad (1.6)$$

where C is a strength parameter, $Q=\frac{1}{2}(k+k')$, and k,i and k',j the four-momenta and isospin indicies of the incoming and outgoing pion, respectively. If the contact term (1.6) is added to the nucleon Born terms [the N and crossed N pole terms shown in Figs. 1(a) and 1(e)] computed from the coupling (1.5), the resulting πN amplitude is *independent of* λ if the external nucleons are on shell, there are no form factors, and $C=1$. This comes about because the contact term in Eq. (1.6) also depends on the mixing parameter λ. It is pure σ-like if the πN coupling is pure γ^5 (corresponding to $\lambda=1$) and pure ρ-like if the πN coupling is pure $\gamma^5\gamma^\mu$ (corresponding to $\lambda=0$), and these contributions are just what is needed to cancel the λ dependence which arises from the nucleon Born terms, giving amplitudes *independent of* λ. However, if these amplitudes are used as driving terms in an integral equation in which the nucleons are off shell, they will no longer give identical results, and it is natural to ask whether a particular choice of λ is favored by the physics.

It was found recently [10,11] that relativistic NN scattering, in a formalism in which one nucleon is off shell, is very sensitive to the mixing parameter λ, and that a very good fit to NN data could be obtained using a one boson exchange (OBE) model with only the four mesons π, σ, ρ, and ω, *provided the* πN *coupling included an admixture of 22%* γ^5 *coupling*. Furthermore, this admixture of pseudoscalar coupling also gives a good description of the p ^{40}Ca spin observables [29]. And recently Goudsmit, Leisi, and Matsinos [30] analyzed πN scattering at the tree level and found that an admixture of about 24% γ^5 gives a good description of the scattering lengths. They obtained this value of the admixture from their analysis of data on pionic atoms with isoscalar nuclei using a relativistic mean field theory.

To get a feeling for the dependence of our model on the parameter λ, we plot the isospin-even scattering length a_+ versus the isospin-odd scattering length a_- in Fig. 3. For convenience, both scattering lengths have been made dimensionless by multiplying by the pion mass μ. Three analyses of the experimental results, labeled I [31], II [32], and III [33], are shown in the figure. The dashed line shows how the scattering lengths, as calculated from the nucleon Born terms only [Figs. 1(a) and 1(e)] vary with the mixing parameter λ. Note that the curve comes closest to the data if $\lambda\cong 0.2$. The solid line gives the dependence of the scattering lengths on λ when the nucleon Born terms are used for the kernel of our πN integral equation, and we see that the iteration of the Born terms by the equation produces negligible effects. From this figure it is clear that if we use a kernel with nucleon Born terms only, pure pseudoscalar coupling ($\lambda=1$) or pure pseudovector coupling ($\lambda=0$) will not give as good a *simultaneous* description of the even and odd scattering lengths as a choice $\lambda\sim 0.2$. Since the OBE model of Ref. [10,11] is most consistent with a model of πN scattering based only on the nucleon Born terms, this result may partially explain why the result $\lambda\cong 0.22$ was obtained.

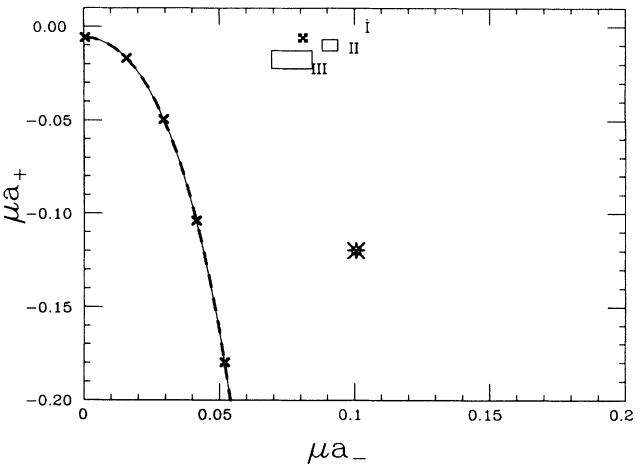

FIG. 3. S-wave π-N scattering lengths. The ×'s on the curves mark values of λ incremented by 0.1, with $\lambda=0$ at the top left end of the curves.

Next, consider a slightly more complete model in which the driving terms of the integral equation include the contact terms of Eq. (1.6), in addition to the nucleon Born terms. Now the Born term result for the scattering lengths is independent of λ, but it turns out that the scattering lengths obtained by solving the integral equation (the cross in Fig. 3) are also (nearly) independent of λ. Finally, the scattering lengths obtained from the solution of the integral equation with the full kernel, including all the terms shown in Fig. 1, also does not depend very much on λ. These results are represented by the large star burst in Fig. 3. We therefore conclude that the scattering lengths (and most of the low energy observables) will be insensitive to λ if the kernel is chirally symmetric.

Does it follow, therefore, that the mixing parameter λ plays no role in the description of πN scattering? To the level of sophistication to which we are working, this is not the case. To see where the dependence on λ reappears, consider the nucleon self-energy $\Sigma(p)$.

D. Nucleon self-energy

If the Roper contributions are omitted for simplicity (they are discussed in detail in Sec. III D), our integral equation produces a nucleon self-energy which can be written diagrammatically as shown in Fig. 4. The elementary pion-nucleon bubble diagram is shown in Fig. 4(a), and all other contributions which come from iter-

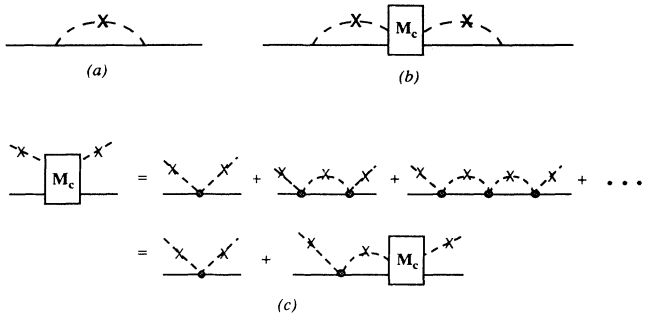

FIG. 4. Diagrams (excluding Roper contributions) which contribute to the nucleon self-energy in this model. (a) Bubble diagram, (b) contributions from connected pieces, with M_c given by the iteration, or integral equation shown in (c).

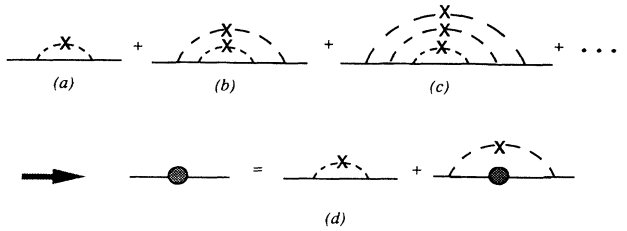

FIG. 5. Infinite subclass of diagrams not included in our model. (a) is included, but its iterations (b), (c), . . ., are not included. All of these diagrams are summed by the integral equation shown in (d).

ating the contact terms are shown in Fig. 4(b). [The integral equation for the unitarized contact amplitude M_c is shown in Fig. 4(c).] Now the contributions shown in Fig. 4 include much physics, but also leave out many processes. An infinite class of diagrams excluded from our model is shown in Fig. 5. As the figure shows, this class could also be summed by the integral equation shown diagrammatically in Fig. 5(d). We can allow for these contributions *approximately* if we demand that, *at the nucleon pole*, the nucleon mass *not be shifted by the interactions*. This requirement means that the infinite family of interactions is, in effect, included automatically, at least near the pole. It also means that the addition of the nucleon self-energy to a model with bare nucleons will produce the minimum effect possible, meaning that the model is fairly stable under changes in the dynamics. We will impose this requirement on our model, and will refer to it as the *stability condition*.

At the nucleon pole the nucleon self energy is only a function of the parameters of the model, and its dependence on the parameter λ (with the others held fixed) is shown in Fig. 6. Note that it is zero for a $\lambda \cong 0.25$, and our stability condition is therefore realized practically as a *constraint* on the parameter λ. Note that this constraint yields a value for λ which is in rough agreement with the value required to simultaneously minimize the error in the scattering lengths a_+ and a_- obtained from the naive model which used only the nucleon poles as the driving term in the integral equation (recall the results shown in Fig. 3 and the subsequent discussion). We do not believe that this is an accident; the value of $\lambda \cong 0.2$ which seems to stabilize the model should also give the best physical approximation in situations where the model is incomplete.

Before leaving this section, we wish to emphasize that the stability condition can only be satisfied if a mixed coupling is used, and that it is almost completely determined by the bubble diagram shown in Fig. 4(a). For pure pseudoscalar coupling, the self-energy is positive definite, while for pure pseudovector coupling it is negative definite, so that only the parameter λ can be determined from the stability condition.

E. Description of spin $\frac{3}{2}$ particles

It is well known that the $\Delta(1232)$ isobar plays an important role in describing interactions involving nucleons, and there are many works which include this resonance. However, in spite of the number of papers which have studied this particle, there is still some disagreement about the best way to describe a spin 3/2 particle, and in this section we will discuss the choice we have adopted. The same choice is used for the D_{13} resonance.

There are two spin 3/2 propagators used in the literature. One, which is known as the Rarita-Schwinger propagator, has the form

$$P'_{\mu\nu} = \left(\frac{i}{M-P}\right)\left[g_{\mu\nu} - \frac{1}{3}\gamma_\mu\gamma_\nu - \frac{2P_\mu P_\nu}{3M^2} - \frac{\gamma_\mu P_\nu - P_\mu\gamma_\nu}{3M}\right], \quad (1.7)$$

where P_μ is the four-momentum of the particle and M its mass. This propagator, which was proposed by Fierz

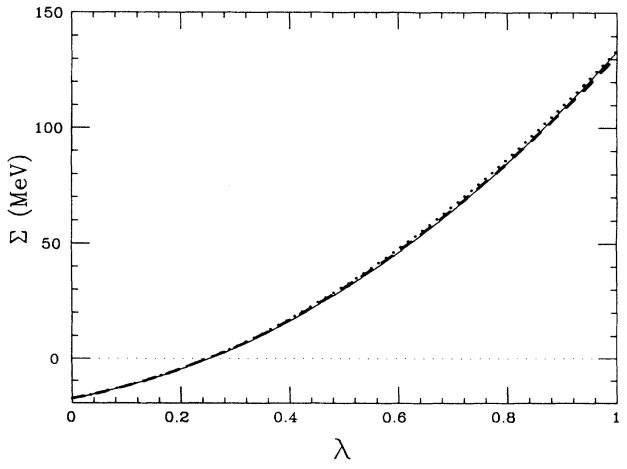

FIG. 6. Self-energy of the nucleon (at the nucleon pole) as a function of λ. The three curves which are practically indistinguishable are the contribution of the bubble diagram only (dashed line), bubble plus nucleon contact terms (dotted line), and the total result.

and Pauli [34] and simplified by Rarita and Schwinger [35] more than 50 years ago, can be obtained from the Lagrangian for a spin 3/2 particle [6, 14]. Another propagator

$$P_{\mu\nu} = \left(\frac{i}{M-\not{P}}\right)\left[g_{\mu\nu} - \frac{1}{3}\gamma_\mu\gamma_\nu - \frac{1}{3P^2}(\not{P}\gamma_\mu P_\nu + P_\mu\gamma_\nu\not{P})\right] \quad (1.8)$$

was recently popularized by Williams [13] and used by Jaus and Woolcock [36], who point out that the Rarita-Schwinger propagator $P'_{\mu\nu}$ projects out a pure spin 3/2 state only when $P^2 = M^2$ (when the particle is on its mass shell). Moreover, Benmerrouche, Davidson, and Mukhopadhyay [14] have recently pointed out that $P_{\mu\nu}$ does not have an inverse, and claim that $P'_{\mu\nu}$ is therefore the correct spin 3/2 propagator.

In this paper we are not interested in developing a field theory of spin 3/2 particles. Instead, we need a propagator which gives a covariant, phenomenological description of a composite spin 3/2 state. Iteration of this term by our integral equation will then generate a dressed contribution which satisfies unitary and has the correct width as determined by the dynamics. We will use the Williams propagator for this purpose, because it turns out to have a very nice property: When iterated by the integral equation, it retains its structure, giving a dressed propagator of the form

$$P^{\text{dressed}}_{\mu\nu} = \left(\frac{i}{M-\not{P}+\Sigma_\Delta(P)}\right) \times \left[g_{\mu\nu} - \frac{1}{3}\gamma_\mu\gamma_\nu - \frac{1}{3P^2}(\not{P}\gamma_\mu P_\nu + P_\mu\gamma_\nu\not{P})\right], \quad (1.9)$$

where $\Sigma_\Delta(p)$ is the self-energy of the Δ. With our kernel, this self-energy turns out to be a simple function. See the discussion in Sec. III E for more details.

F. The Roper

The P_{11} phase shift is small and negative at low energy; then it changes sign at $T_\pi \sim 150$ MeV and grows rapidly to pass through a resonance [$N^*(1440)$] at $T_\pi \sim 485$ MeV. There are two different explanations for this behavior in the literature. Oset, Toki, and Weise [17] argue that the Roper is needed to change the sign of the P_{11}, which is negative at low energies because of the nucleon pole term. However, Mizutani *et al.* [15], Morioka and Afnan [16], and Pearce and Jennings [9] argue that this sign change is due to a cancellation between the repulsion from the nucleon pole and attractive nonpole contributions, and can be understood without the Roper. Our calculation supports this latter point of view, as we will show later.

In this paper we study the role of the N^* both at low energy and in the resonance region. To describe the N^* consistently, we include a new "nucleon" pole term with a mass m^* in the kernel of the integral equation, and iterate these contributions to all orders (in the same way other contributions are handled), being careful to include contributions from the amplitudes which describe the transition of a Roper to a nucleon, and vice versa. We describe the principal inelastic channel of the Roper by including the inelastic transitions $N^* \to \pi + \Delta$ and $\pi + \Delta \to N^*$. The final solution satisfies unitarity, and automatically dresses the Roper pole. This treatment is discussed in detail in Sec. III D.

G. Results

Our principal results are shown in Figs. 7–15 and Table I. The S-, P-, and D-wave phase shifts and inelasticities are shown in Figs. 7–13, the total elastic $\pi^- p$ cross section in Fig. 14, and the total elastic $\pi^+ p$ cross section in Fig. 15. In each of these figures, the solid line is the total result, including all of the driving terms shown in Fig. 1. Our fit to the phase shifts and inelasticities is very good, with an overall $\chi^2 \simeq 1.7$ per phase point.

Table I gives the final values of all parameters. Those given in boldface (14 parameters) were *adjusted* to make the fit. The πNN coupling constant was initially fixed at the value shown, but later we did try varying it and found that the fit could not be significantly improved and was not very sensitive to small variations in its value. The Table also gives values of parameters *determined* by the fit. These include *effective* resonance masses and widths (see below) and two other parameters *fixed* by consistency requirements. The πNN mixing parameter λ was determined by the requirement that the nucleon mass be unshifted by the interaction, as discussed above, and the overall strength C of the combined σ- and ρ-like contact terms [recall Eq. (1.6)] was fixed so as to ensure that they exactly cancel the nucleon pole terms at

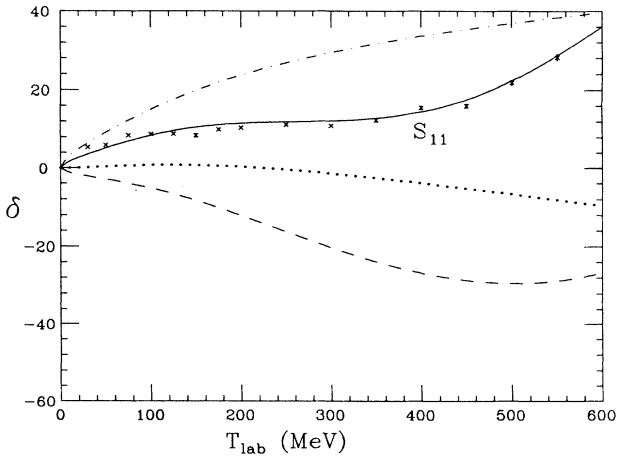

FIG. 7. Fits to the S_{11} phase shift. As explained in the text, the dotted line is the nucleon Born terms only, the dot-dashed line is the addition of the σ- and ρ-like contact terms required by chiral symmetry, the dashed line adds in the N^* contributions, and the solid line is the total result, obtained by adding the additional ρ-like contact term.

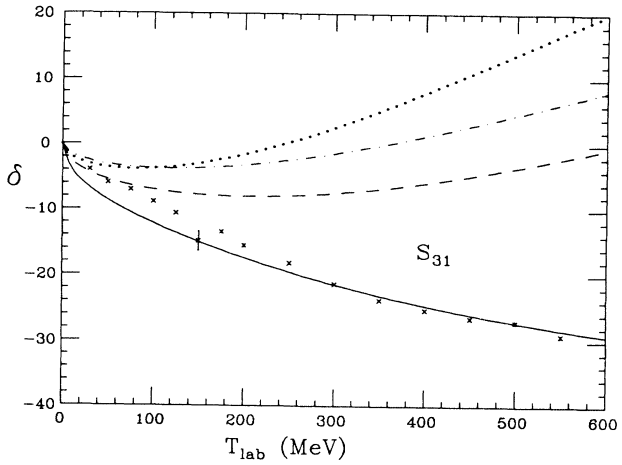

FIG. 8. Fits to the S_{31} phase shift. The curves are the same as in Fig. 7.

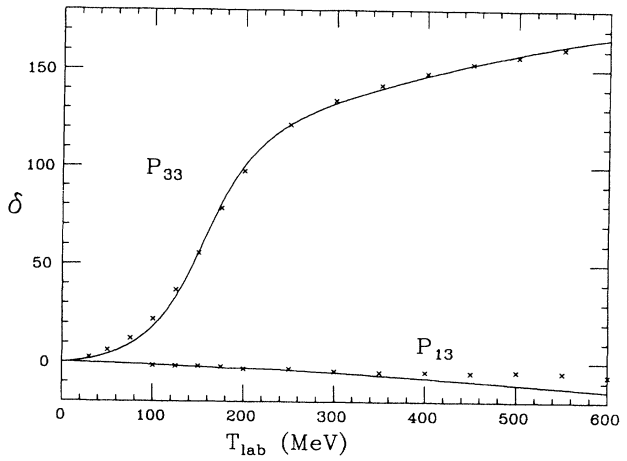

FIG. 11. Fit to the isospin 3/2 P-wave phase shifts.

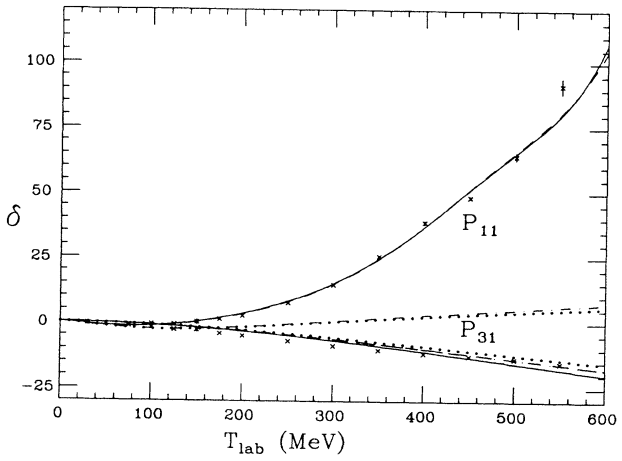

FIG. 9. Fits to the isospin 1/2 P-wave phase shifts.

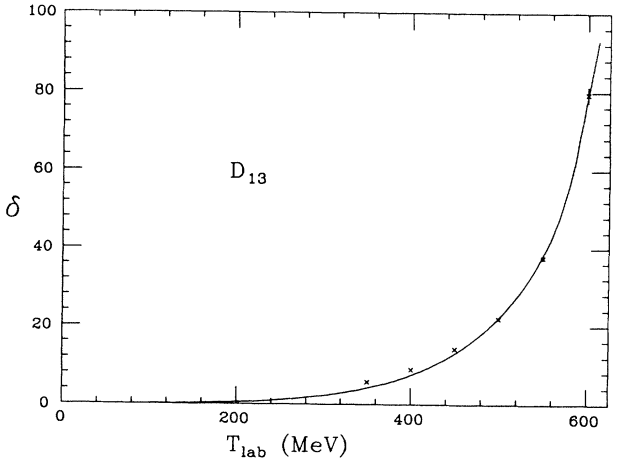

FIG. 12. Fit to the D_{13} phase shift.

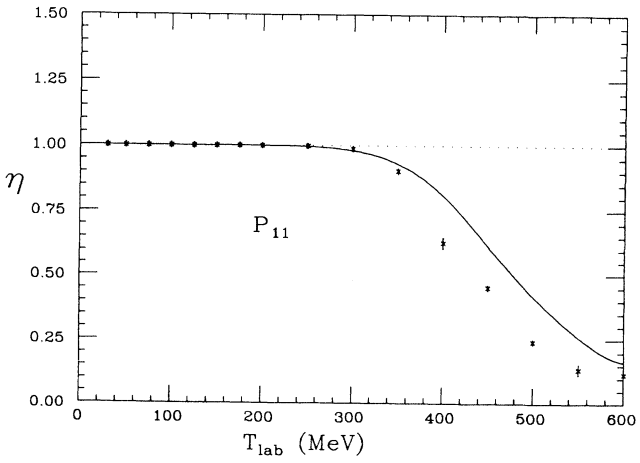

FIG. 10. P_{11} inelasticity parameter.

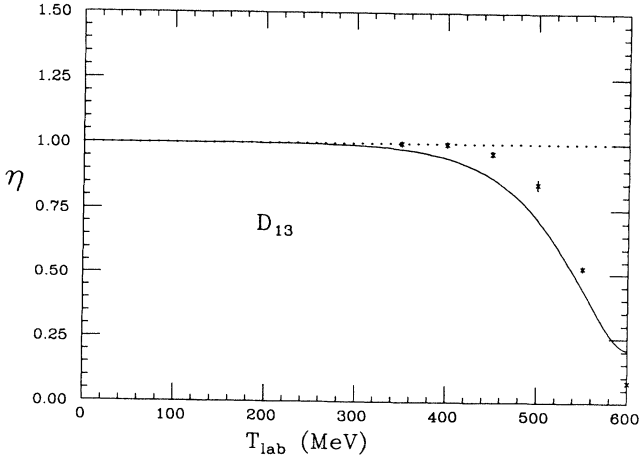

FIG. 13. D_{13} inelasticity parameter.

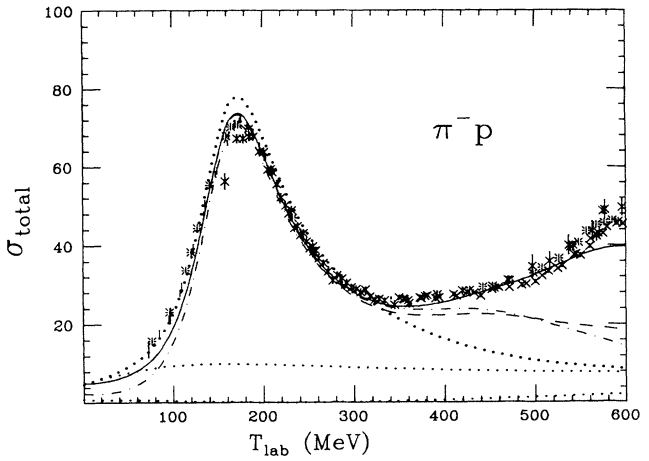

FIG. 14. Fits to the $\pi^- p$ total cross section.

the πN threshold, as *required* by chiral symmetry. (This adjustment is necessary because the nucleon form factors are not unity at the πN threshold.)

Because of our choice of spin 3/2 propagator, and our approximation scheme which leads to the result that the crossed Δ and D_{13} poles are zero when approximated as contact terms (for details see the discussion in Sec. III), the Δ contributes *only* to the P_{33} channel (except for a tiny contribution to the D_{33} channel, which we will not discuss), and the D_{13} contributes *only* to the D_{13} and P_{13} channels. Furthermore, approximating the crossed nucleon and Roper poles by contact terms means that they *only* contribute to spin 1/2 channels. Hence the phase shifts decouple, with the P_{33} channel driven only by the direct Δ pole, the D_{13}-P_{13} channels driven only by the direct D_{13} pole, and all the other (spin 1/2) channels driven only by the nucleon N^* and the effective σ- and ρ-like contact terms.

It is therefore convenient to describe the fits to each of the decoupled channels separately, and we will begin with the spin 1/2 channels, shown in Figs. 7–10. As discussed above, these channels are driven by the nucleon and N^* Born terms, and the effective σ- and ρ-like contact terms. These driving terms depend on only eight adjustable parameters: the undressed mass of the N^* pole, m^*, the bare πNN^* coupling g_{N^*}, the strength of an "additional" ρ-like $\pi\pi NN$ contact term V_ρ not required by (but consistent with) chiral symmetry, parametrized by a constant C_ρ, where (omitting the form factors)

$$V_\rho \simeq -C_\rho \frac{g^2}{4m^2}[\tau_j, \tau_i]\not{Q} \ , \tag{1.10}$$

three parameters needed to describe the inelasticity of the N^*, and two form factor masses: the mass in the nucleon form factor Λ and the mass in the N^* form factor Λ^*.

The inelasticity of the N^* is approximately described by coupling to the $\pi\Delta$ channel, with coupling constant g'_{N^*}. Now the Δ which dominates the P_{33} channel is fully dressed by the interactions, but for simplicity, we did not dress the delta in the $\pi\Delta$ inelastic channel, and we compensate for this omission by allowing this virtual, undressed delta, which we denote by Δ' to have a different mass $m_{\Delta'}$ and form factor with a different functional form and mass, $\Lambda_{\Delta'}$. We find that the fit to the Roper inelasticity, shown in Fig. 10, requires $m_{\Delta'} = 1074$ MeV. This low value is close to the sum $m + \mu = 1078$ MeV, showing that a good description of the inelasticity requires that the $N\pi\pi$ threshold be in the right place. This leads us to believe that our model can be improved by replacing this effective delta with the fully dressed delta determined from the fit to the P_{33} channel.

Before we discuss the fits to the other channels, we wish to point out that the S waves, shown in Figs. 7 and 8,

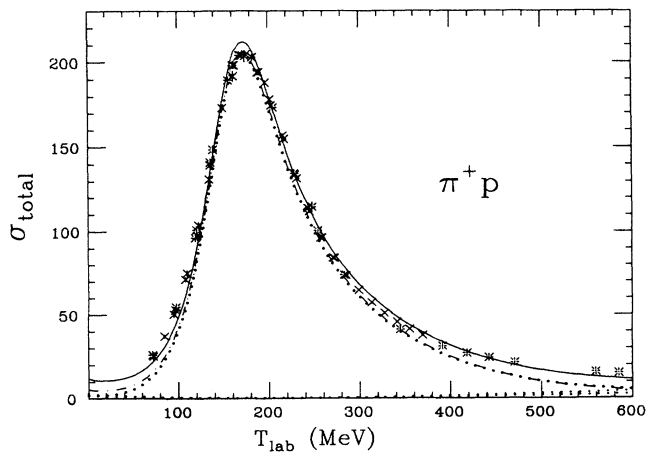

FIG. 15. Fits to the $\pi^+ p$ total cross section.

TABLE I. Parameters of the model. Those in boldface were varied during the fit; the others are determined by the fit.

Parameter	Bare	Dressed
$g^2/4\pi$	13.5	12.72
λ	0.253	
C	0.891	
C_ρ	**0.903**	
m^*	**1444.7**	1456.0
$g^2_{N^*}/4\pi$	**4.792**	6.857
Γ^*		265.9
$Z(m)$		−0.019
$Z(m^*)$		$-0.023i-0.046i$
$m_{\Delta'}$	**1074.4**	
$g'^2_{N^*}/4\pi$	**0.031**	
Λ	**1294.3**	
Λ^*	**1951.7**	
$\Lambda_{\Delta'}$	**1092.1**	
m_Δ	**1318.6**	1229.1
$g^2_\Delta/4\pi$	**0.459**	0.365
Γ_Δ		109.8
Λ_Δ	**1506.2**	
m_D	**1513.4**	1518.6
$g^2_D/4\pi$	**0.346**	0.974
Γ_D		179.0
$g'^2_D/4\pi$	**0.073**	

are particularly sensitive. To show how the total result is built up from individual contributions, the curves in the figures show the result when the kernel (i) includes only the direct nucleon pole term and the contact term derived from crossed nucleon exchange (the dotted line), (ii) the terms in (i) *plus* the combined σ- and ρ-like contact terms of Eq. (1.6) (the dot-dashed line), (iii) the terms in (ii) *plus* N^* driving terms (the dashed line), and finally (iv) the total result, which includes the terms in (iii) *plus* the additional ρ-like $\pi\pi NN$ contact term of Eq. (1.10) (the solid line). Since the contributions add nonlinearly, it is difficult to extract the separate contributions from the figures, but we can conclude that the chiral model without the N^* and rho [(ii)] gives a very good account of the scattering lengths, but the N^* pushes the S_{11} phase shift in the wrong direction, and only after the additional rho is added do we restore the correct low energy behavior. The bend in the S_{11} is due to the N^*, and we have no need for the $S_{11}(1535)$ in our model.

The same curves are shown for the spin 1/2 P waves in Fig. 9. Note that the nucleon Born terms make a very small contribution to the P_{11} channel above 200 MeV, but that below 200 MeV they already exhibit the change from repulsion to attraction. The Born terms alone give a zero in the P_{11} phase shift at $\simeq$ 280 MeV, but inclusion of the Roper moves this zero down to the correct region $\simeq$ 150 MeV. At higher energies the P_{11} phase shift is dominated by the Roper, with the contributions from the σ- and ρ-like contact terms being very small.

We now discuss the spin 3/2 channels, where the situation is much simpler. The results for the P_{33} channel are shown in Fig. 11. This channel is fit by three parameters: the bare delta mass m_Δ, the bare $\pi N\Delta$ coupling constant g_Δ, and a mass in the delta form factor Λ_Δ. (The nucleon form factor has already been fixed by the fit to the spin 1/2 channels.) Note that the mass of the bare, unshifted delta pole is at 1319 MeV, considerably higher than the nominal delta mass of 1232 MeV, but that the dressed Δ mass is very close to the nominal value of 1232.

The D_{13}-P_{13} channels are fit by three more parameters: the bare mass of the D_{13} pole, m_D, the coupling of the D_{13} to the πN channel, g_D, and the coupling of the D_{13} to the inelastic $\pi\Delta'$ channel, g'_D, which describe the inelasticity of the D_{13} approximately. The parameters which describe the effective delta in the inelastic channel, $m_{\Delta'}$ and $\Lambda_{\Delta'}$, are constrained to be identical to those used for the Roper. The fit to the D_{13} channel, shown in Figs. 12 and 13, is good, and the bare D_{13} mass m_D is about 1513 MeV, in good agreement with the nominal value of 1520 MeV.

The total elastic $\pi^- p$ cross section is shown in Fig. 14. The data are from Ref. [31]. The three dotted curves are the result for a kernel with nucleon Born terms only (practically zero), the Born terms plus the chiral contact terms, and then these with the Δ contribution. The Δ clearly dominates the cross section below 300 MeV. The addition of the N^* (the dot-dashed line) followed by the additional rho (the dashed line) suppresses the cross section up to 300 MeV, but gives needed strength above 400 MeV, and adding the D_{13} to get the final result (solid line) restores the cross section at very low energies and gives a very significant addition above 400 MeV.

The total elastic $\pi^+ p$ cross section is shown in Fig. 15. The two dotted curves which are practically zero are the result for a kernel with nucleon Born terms only and Born terms plus chiral contact terms. Then the results of adding the Δ and the crossed N^* are two overlapping dotted and dot-dashed curves. Finally, the addition of the extra rho (solid line) makes small but important contributions at low and high energies.

A number of interesting parameters are determined by our fits, and these are also given in Table I. We have already discussed how the πN mixing parameter λ is fixed by the *stability condition*, and how the strength of the λ-dependent σ- and ρ-like contact terms, defined in Eq. (1.6), is fixed by chiral symmetry. In addition, we have looked at our solutions, and extracted an *effective* mass and width for each resonance by writing the solutions, near the resonance, in the approximate form

$$M = \frac{A}{m_{\text{eff}} - W - i\frac{1}{2}\Gamma} + B \quad , \tag{1.11}$$

where m_{eff} and Γ are constants obtained from the exact solutions (which depend on the total c.m. energy W) *evaluated at* $W = m_{\text{eff}}$. In particular, the value of m_{eff} is the solution of the nonlinear equation

$$m_R - m_{\text{eff}} + \text{Re}\Sigma_R(m_{\text{eff}}) = 0 \quad , \tag{1.12}$$

where m_R is the bare mass and $\Sigma_R(W)$ is the self-energy of the resonance R. The values of these *effective* masses and widths are given in Table I. The definition of the effective coupling constants for the resonances, g_{eff}, is discussed in Appendix D. The renormalized πNN coupling constant g^R is

$$\left(\frac{g^R}{g}\right)^2 = \left(1 - \frac{\partial}{\partial W}\Sigma_N(W)\right)^{-1}\Bigg|_{W=m} \quad . \tag{1.13}$$

Note that the renormalization of the πNN coupling constant is not insignificant.

The coupling of the nucleon to the N^* means that the dressed states are linear combinations of the bare nucleon and N^* states. The admixture is given by a function $Z(W)$ [defined in Eq. (3.27)], and the values of Z at the nucleon mass and at the effective N^* mass are given in Table I. Note that the mixing is only a few percent.

Finally, we close this review of our results by discussing the form factors used in this model (for a detailed discussion, see Sec. III C). A form factor is needed to ensure that the solutions of the integral equation exist, or alternatively, to cut off the integrals over the πN loops which appear in the solution. This form factor cannot be associated with the pion mass, as is usually done in pion exchange models, because the pion is on shell. Anticipating the extension of this model to the description of the electroproduction of pions, where a gauge invariant treatment of electromagnetic interactions is possible following the procedure introduced in Ref. [37], we choose to make the form factor depend only on the off-shell nucleon mass, and to identify the form factor with the nucleon itself, so

that the same universal form factor will be used for all off-shell nucleons, wherever they appear. When the nucleon form factor accompanies the intermediate nucleon in the direct nucleon pole term, the virtual nucleon mass (squared) is simply

$$W^2 = m^2 + \mu^2 + 2m(T_{\rm lab} + \mu) \ , \tag{1.14}$$

and the form factor is plotted versus $T_{\rm lab}$ in Fig. 16. When the nucleon form factor accompanies a virtual nucleon in a πN loop, its mass (squared) is

$$p^2 = W^2 + \mu^2 - 2W\omega(k) \ , \tag{1.15}$$

where k is the magnitude of the pion three-momentum in the loop, and $\omega = \sqrt{\mu^2 + k^2}$. The form factor is plotted versus k for a fixed $W = m + \mu$ in Fig. 17. We emphasize that the *same* nucleon form factor is shown in both figures; only the variable on which it depends has been changed.

Because of the inelastic $\pi\Delta'$ channel, a form factor is also needed for the Δ', and once form factors have been introduced for the nucleon and delta, it is natural to include form factors for the other resonances as well. We found that no form factor was needed for the D_{13}, but an N^* form factor was included because it improved our fits. The Δ and N^* form factors are plotted versus $T_{\rm lab}$ for the kinematics of Eq. (1.14) in Fig. 16. In common with the nucleon form factor, the Δ and Δ' form factor was also chosen to peak at the nucleon mass m, but the N^* form factor was chosen to peak at the N^* mass. The Δ' form factor is plotted in Fig. 17 for the appropriate kinematics of Eq. (1.15), but with $W = m_{\Delta'} + \mu$. Unfortunately, our results are sensitive to the form factors, which are purely phenomenological.

H. Conclusions

We draw the following conclusions from this work.

A simple resonance pole model, with nucleon, delta, Roper, and D_{13} poles and other couplings described by 14 adjustable parameters (including 4 resonance masses, 6 coupling constants, and 4 form factor masses) has been found to give a very good description of πN scattering up to pion laboratory energies of 600 MeV. The model is simple, covariant, satisfies unitarity exactly, and is approximately chirally symmetric at threshold. A very good description of the data up to 400 MeV laboratory energy would require only 8 parameters.

The requirement that the nucleon mass be unshifted by the interaction (referred to as the *stability condition*) can be satisfied only if the πN coupling is a mixture of pseudoscalar and pseudovector couplings, and the value we obtain (25% pseudoscalar and 75% pseudovector) is well constrained by our fit, and largely independent of the values of the other parameters. Furthermore, it is in good agreement with the value of this parameter obtained from a OBE model of NN scattering [10].

The spin 3/2 resonances in our model have no virtual spin 1/2 components, leading us to conclude that such components (which may very well be present in a less phenomenological treatment) are not necessary for a successful fit to the data.

The position of the bare Δ pole ($m_\Delta \simeq 1319$ MeV) is surprisingly far from the effective mass of the Δ resonance ($m_\Delta^{\rm eff} \simeq 1230$ MeV). This should be taken into account in any quark model which neglects pion interactions. The same is not true for the Roper and the D_{13}; in these cases the bare and effective masses are quite close to each other.

The existence of a zero in the P_{11} phase shift does not depend on the Roper, but its precise location is sensitive to the presence of a Roper resonance.

The value of the renormalized πNN coupling constant, $(g^R)^2/4\pi$, is not well determined by our model; a good fit is obtained for values in the range 12–15.

The remainder of this paper is divided into two parts, which give more details about the relativistic wave equation which we use, and the details of the model.

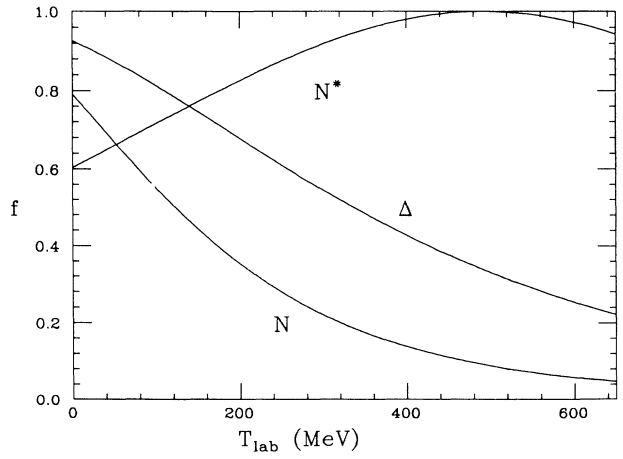

FIG. 16. Form factors for the nucleon, Roper, and Δ.

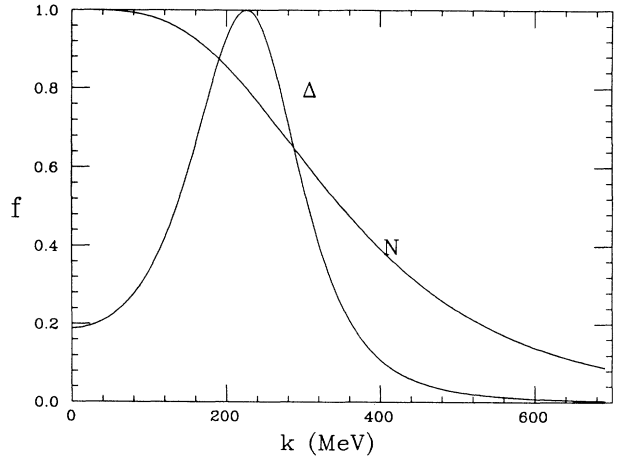

FIG. 17. Form factors for the nucleon and Δ' plotted as a function of the pion loop momentum.

II. GENERAL THEORY

In this part the relativistic equation for the πN scattering matrix $\mathbf{M}$ is presented, and we show that the theory is covariant and satisfies unitarity. We include a complete discussion of the justification for restricting the pion to its mass shell. Then we develop the technique used to solve the integral equations.

A. Why should the pion be on shell?

Before we construct the covariant integral equation used to describe πN scattering, we discuss typical Feynman diagrams which contribute to the scattering amplitude. Following the historical route, we first consider a *simplified* problem where πN scattering is dominated by diagrams such as the direct and crossed nucleon poles [diagrams (a) and (e) in Fig. 1]. A unitarized amplitude is obtained from these "driving terms" by iterating them to all orders. (The role of the integral equation is to carry out this iteration in a convenient, closed form.) The iteration of the direct pole diagrams [Fig. 1(a)] is straightforward; the most challenging case is the iteration of the crossed nucleon pole diagrams [Fig. 1(e)] and we are therefore led to look at the diagram in Fig. 18(a) and the corresponding crossed diagram shown in Fig. 18(b). The box and crossed box diagrams, which occur in the meson exchange theory, are shown in Figs. 19(a) and 19(b) for comparison, and will also be reviewed below.

For simplicity, we will carry out our analysis at threshold, with all of the external particles on shell, so that the four-momenta of the external nucleons is $p_0 = (m, \mathbf{0})$, and of the external pions is $q_0 = (\mu, \mathbf{0})$. The four-momentum of the internal pion is $k = (k_0, \mathbf{k})$, and each of the diagrams (18) have four poles and two double poles in the complex k_0 plane. If the three-momentum $\mathbf{k}$ is very small, the location of these poles is as shown in Fig. 20, and introducing the quantities $\omega = \sqrt{\mu^2 + \mathbf{k}^2}$ and $E = \sqrt{m^2 + \mathbf{k}^2}$, the poles for the box [Fig. 18(a)] are at

$$
\begin{aligned}
k_0^{1a} &= \omega - i\epsilon, \\
k_0^{2a} &= m + \mu - E + i\epsilon, \\
k_0^{3a} &= m - E + i\epsilon, \\
k_0^{4a} &= -\omega + i\epsilon, \\
k_0^{5a} &= E + m - i\epsilon, \\
k_0^{6a} &= E + m + \mu - i\epsilon \ .
\end{aligned}
$$

Since $m > \mu$, the poles (5a) and (6a) will give very small

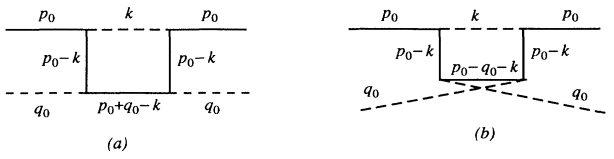

FIG. 18. Feynman diagrams used to construct the integral equation for πN scattering.

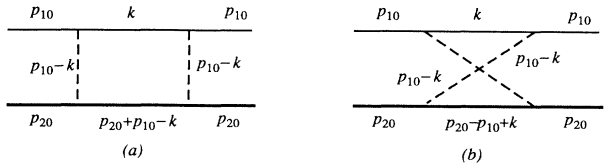

FIG. 19. Feynman diagrams used to construct the integral equation for the scattering of two heavy particles exchanging a light meson.

contributions, and we see that the box is *very well approximated* by closing the k_0 contour in the lower half plane, and *keeping only the positive energy pion pole* (1a). The *same* argument holds for the "crossed box" [Fig. 18(b)] with singularities at

$$
\begin{aligned}
k_0^{1b} &= \omega - i\epsilon, \\
k_0^{2b} &= m - \mu - E + i\epsilon, \\
k_0^{3b} &= m - E + i\epsilon, \\
k_0^{4b} &= -\omega + i\epsilon, \\
k_0^{5b} &= E + m - i\epsilon, \\
k_0^{6b} &= E + m - \mu - i\epsilon \ .
\end{aligned}
$$

Note that only the poles (2) and (6) have a location different for the corresponding poles in (a), and that the pole in the lower half plane, (6), is still quite distant from the pole (1), which gives the dominant contribution.

We can use this analysis to make some very interesting estimates. If the pion three-momentum is small, so that $E \simeq m$, then the contribution from the dominant pion pole (1) to the box (a) and crossed box (b) is approximately

$$
\mathbf{M}_\pi^a = \frac{1}{(\omega - \mu)(2\omega^3)(8m^3)} \quad \mathbf{M}_\pi^b = \frac{1}{(\omega + \mu)(2\omega^3)(8m^3)} \ , \tag{2.1}
$$

and the contributions from the poles (5) and (6) are approximately

$$
\mathbf{M}_m^a = \mathbf{M}_m^b = \frac{15}{(2m)^7} \ . \tag{2.2}
$$

From these we conclude the following. If we neglect the crossed box, we make an "error" proportional to

$$
\frac{\mathbf{M}^b}{\mathbf{M}^a} = \frac{\omega - \mu}{\omega + \mu} \ . \tag{2.3}
$$

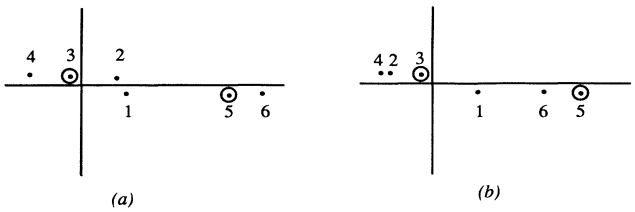

FIG. 20. Pole structure of the diagrams in Fig. 18.

Since momenta of the order of a few hundreds of MeV are probably important, the crossed box contributions are not negligible when compared with the box contributions generated by the iteration of the crossed nucleon pole term. But these crossed boxes will not be included in our kernel, and hence our calculation of the effects of the crossed nucleon driving term is intrinsically approximate. Approximating the crossed nucleon driving term by a contact term is therefore not inconsistent with the precision of this method. The "error" which results from neglecting the two poles (5) and (6) is negligible:

$$\frac{\mathbf{M}_m^a}{\mathbf{M}_\pi^a} \sim \frac{(\omega-\mu)\omega^3}{m^4} \quad . \tag{2.4}$$

Therefore, the difference between the use of the Bethe-Salpeter equation and our equation in which the pion is on shell is not large enough to justify the difficulty which accompanies a serious attempt to solve the Bethe-Salpeter equation. This is particularly true in view of the fact that a much larger error results from the neglect of the crossed box terms, which are neglected in both methods.

The conclusion that the *light* particle (the pion) should be put on shell is very different from the result obtained in a theory in which a light meson is exchanged between heavy particles with masses m_1 and m_2, where both m_1 and m_2 are much greater than μ. If we take $m_2 > m_1$, then the best approximation leads to an equation in which the *heavy* particle (m_2) is on shell [24], and it is worthwhile to review the difference between these two cases here. The box and crossed box for the meson exchange case (Fig. 19) also have four poles and two double poles in the complex k_0 plane, with the singularities as shown in Fig. 21. If we take m_2 to be very large, so that $E_2 = \sqrt{m_2^2+\mathbf{k}^2} \simeq m_2$, then the singularities of the box are at

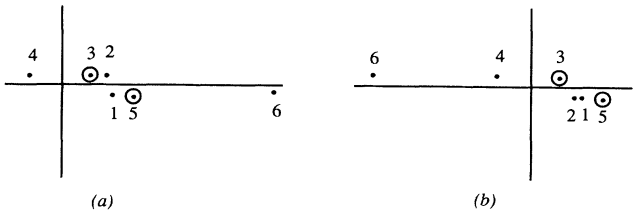

FIG. 21. Pole structure of the diagrams in Fig. 19.

$$\begin{aligned} k_0^{1a} &= E_1 - i\epsilon, \\ k_0^{2a} &= m_1 + i\epsilon, \\ k_0^{3a} &= m_1 - \omega + i\epsilon, \\ k_0^{4a} &= -E_1 + i\epsilon, \\ k_0^{5a} &= m_1 + \omega - i\epsilon, \\ k_0^{6a} &= 2m_2 + m_1 - i\epsilon \quad , \end{aligned}$$

where $E_1 = \sqrt{m_1^2+\mathbf{k}^2}$ and $\omega = \sqrt{\mu^2+\mathbf{k}^2}$. Because the exchanged particle is *light*, the situation is *completely different*; while the poles at (1) and (2) dominate, the singularities from the exchanged meson are very close, and are the most important source of "error." Because the singularity at (5) is now very close to (1), the "light" particle pole at (1) no longer clearly dominates. Here the crossed box plays an important role. As before, its singularities are at the same places as the box, *except* for the poles at (2) and (6), which are at

$$\begin{aligned} k_0^{2b} &= m_1 - i\epsilon, \\ k_0^{6b} &= m_1 - 2m_2 + i\epsilon \quad . \end{aligned}$$

Now we see that the crossed box is well approximated by closing the contour in the upper half plane, and keeping only the double pole (3). However, this contribution is *canceled* by a similar contribution from the same pole in the box. Neglecting the distant poles (6) and (4), the sum of the two diagrams is

$$\mathbf{M}^a + \mathbf{M}^b \simeq \int dk_0 \frac{1}{(\omega - m_1 + k_0 - i\epsilon)^2(\omega + m_1 - k_0 - i\epsilon)^2(E_1 - k_0)} \left[\frac{1}{(k_0 - m_1 - i\epsilon)} + \frac{1}{(m_1 - k_0 - i\epsilon)}\right] \quad , \tag{2.5}$$

which displays the cancellation. However, (2.5) is not zero, because the two poles in the bracket "pinch." The only way to evaluate (2.5) exactly, *without considering the crossed box at all*, is to close the coutour in the upper half plane, in which case the total result comes only from the pole (2) in the box, corresponding to putting the *heavy* particle on shell.

Looking back over the arguments in the two cases, we see that the *essential difference is the mass of the exchanged particle.* If this mass is large (which is the case for πN scattering), then the singularities from the exchange are very distant, and the on-shell contributions of the light particle dominate. If the mass is light, the singularities from the exchange are important, and are best canceled by putting the heavy particle on shell, and as the discussion shows [24], the *exact* answer is obtained in the limit when the mass of the heavy particle becomes very large.

B. Integral equation

To obtain the correct factors for our equation, it is convenient to start with the Bethe-Salpeter equation for πN scattering,

$$\mathbf{M}_{\alpha'\alpha}(p',p,P) = \mathbf{V}_{\alpha'\alpha}(p',p,P) + i\int \frac{d^4k}{(2\pi)^4} \mathbf{V}_{\alpha'\alpha''}(p',k,P) G_{B\,\alpha''\alpha'''}(k,P) \mathbf{M}_{\alpha'''\alpha}(k,p,P), \tag{2.6}$$

where $\mathbf{M}_{\alpha'\alpha}(p',p,P)$ and $\mathbf{V}_{\alpha'\alpha}(p',p,P)$ are the scattering matrix and the relativistic kernel (potential) of the scattering, α, α', and α'' are Dirac indicies of the initial, final, and intermediate states, and the two-body propagator $G_{B\,\alpha'',\alpha'''}(k,P)$ is

$$G_{B\,\alpha'',\alpha'''}(k,P) = \frac{(m+\not{P}-\not{k})_{\alpha''\alpha'''}}{(\mu^2-k^2-i\epsilon)[m^2-(P-k)^2-i\epsilon]} \quad . \tag{2.7}$$

The initial and final momenta of the nucleon are denoted by p and p', and the total momentum is P. In center of mass system these momenta are written

$$P=(W,0), \quad p=(W-k_0,-\mathbf{k}), \quad k=(k_0,\mathbf{k}), \quad p'=(W-k'_0,-\mathbf{k}'), \quad k'=(k'_0,\mathbf{k}'), \tag{2.8}$$

where W is the total energy of the system.

Equation (2.6) can be reduced to the three-dimensional equation with the pion on shell by formally integrating over the internal pion energy k_0 and retaining *only* the contribution from the positive energy pion pole in the propagator (2.7), giving

$$\mathbf{M}_{\alpha'\alpha}(p',p,P) = \mathbf{V}_{\alpha'\alpha}(p',p,P) - \int \frac{d^3\mathbf{k}}{(2\pi)^3\,2\omega_k}\mathbf{V}_{\alpha'\alpha''}(p',k,P)g_{\alpha''\alpha'''}(k,P)\mathbf{M}_{\alpha'''\alpha}(k,p,P), \tag{2.9}$$

where the two-body propagator $G_{B\,\alpha''\alpha'''}(k,P)$ is now replaced by the off-shell nucleon propagator $g_{\alpha''\alpha'''}(k,P)$,

$$g_{\alpha''\alpha'''}(k,P) = \frac{[m+(\not{P}-\not{k})]_{\alpha''\alpha'''}}{[m^2-(P-k)^2-i\epsilon]}, \tag{2.10}$$

and $\omega_k = k_0 = \sqrt{\mu^2+\mathbf{k}^2}$ is the on-shell energy of pion.

Consider a kernel which is a sum of a contact term $V_{c\,\alpha'\alpha}(p',p,P)$ and baryon pole terms, collectively denoted by B (the set $\{B\}$ includes the nucleon itself),

$$\mathbf{V}_{\alpha'\alpha}(p',p,P) = V_{c\,\alpha'\alpha}(p',p,P) + \sum_B \Gamma^{0\dagger}_{B\,\alpha'}(p',P)\,G^0_B(P)\,\Gamma^0_{B\,\alpha}(p,P) \quad , \tag{2.11}$$

where $\Gamma^0_{B\,\alpha}(p,P)$ are undressed vertex functions describing the coupling of baryon $B \to \pi N$, $\Gamma^\dagger(p,P) = -C^{-1}\Gamma^T(-p,-P)C$ (where C is the Dirac charge conjugation matrix), and $G^0_B(P)$ are the undressed propagators of the baryons. Then, *if the baryons do not mix*, it can be shown that the solution to (2.9) can be written

$$\mathbf{M}_{\alpha'\alpha}(p',p,P) = \mathbf{M}_{c\,\alpha'\alpha}(p',p,P) + \sum_B \Gamma^\dagger_{B\,\alpha'}(p',P)\,G_B(P)\,\Gamma_{B\,\alpha}(p,P), \tag{2.12}$$

where $\mathbf{M}_{c\,\alpha'\alpha}(p',p,P)$ is the infinite sum of iterated contact diagrams,

$$\mathbf{M}_{c\,\alpha'\alpha}(p',p,P) = \mathbf{V}_{c\,\alpha'\alpha}(p',p,P) - \int \frac{d^3\mathbf{k}}{(2\pi)^3\,2\omega_k}\mathbf{V}_{c\,\alpha'\alpha''}(p',k,P)g_{\alpha''\alpha'''}(k,P)\mathbf{M}_{c\,\alpha'''\alpha}(k,p,P) \ , \tag{2.13}$$

$\Gamma_{B\,\alpha}(p,P)$ is the dressed vertex for baryon B, which is computed from the bare vertex and $\mathbf{M}_c$ using the equation

$$\Gamma_{B\,\alpha}(p,P) = \Gamma^0_{B\,\alpha}(p,P) - \int \frac{d^3\mathbf{k}}{(2\pi)^3\,2\omega_k}\Gamma^0_{B\,\alpha''}(k,P)g_{\alpha''\alpha'''}(k,P)\mathbf{M}_{c\,\alpha'''\alpha}(k,p,P) \quad , \tag{2.14}$$

and $G_B(P)$ is the dressed baryon propagator, which is calculated from the equation

$$G_B(P) = G^0_B(P)\left(\frac{1}{1+G^0_B(P)\,\Sigma_B(P)}\right) \quad , \tag{2.15}$$

where $\Sigma_B(P)$ is the baryon self-energy, given by

$$\Sigma_B(P) = \int \frac{d^3\mathbf{k}}{(2\pi)^3\,2\omega_k}\Gamma^0_{B\,\alpha}(k,P)g_{\alpha\alpha'}(k,P)\Gamma^{0\dagger}_{B\,\alpha'}(k,P)$$

$$- \int\int \frac{d^3\mathbf{k}\,d^3\mathbf{k}'}{(2\pi)^6\,4\omega_k\omega'_k}\Gamma^0_{B\,\alpha}(k,P)g_{\alpha\alpha'}(k,P)\mathbf{M}_{c\,\alpha'\alpha''}(k,k',P)g_{\alpha''\alpha'''}(k',P)\Gamma^{0\dagger}_{B\,\alpha'''}(k',P) + \Sigma^{\text{inel}}_B(P) \quad , \tag{2.16}$$

where $\Sigma_B^{\rm inel}$ contains the effect of the coupling of baryon B to inelastic channels (discussed in Sec. III G). Equation (2.12) is illustrated diagrammatically in Fig. 22, and Eqs. (2.14), (2.15), and (2.16) in Figs. 23(a), 23(b), and 23(c), respectively. The equivalence of Eqs. (2.12)–(2.16) with Eq. (2.9) is proved in Appendix A for the case of a single baryon, and the proof is trivially generalized to more than one if there is no mixing. If there is mixing, which is the case for the nucleon and the Roper, the self-energies and propagators become matrices, and this case is discussed in detail in Sec. III D.

It is more convenient to use Eq. (2.12) instead of Eq. (2.9) for several reasons. (i) Since we approximate the crossed terms by contact terms, all of factors which make up Eq. (2.12) can be expressed as geometric series, and summed to a closed convenient form. (ii) We want to keep the nucleon pole unshifted, and this requirement is conveniently implemented by requiring that Eq. (2.16), for $B = N$, be zero at $P^2 = m^2$. (iii) The form of Eq. (2.12) enables us to separate the resonance contributions from the background, and the widths of resonances can be easily obtained from Eqs. (2.16).

All of the integral equations above are manifestly covariant. This is guaranteed by the covariance of the volume integration,

$$\int \frac{d^3\mathbf{k}}{2\omega_k} = \int d^4k\delta_+(m^2 - k^2). \tag{2.17}$$

Furthermore, these equations automatically give a solution which satisfies unitarity exactly, as we will show in the next section.

C. Unitarity

The derivation of the unitarity relation for pion nucleon scattering is similar to the one given in Ref. [11] for NN scattering.

Let us start from Eq. (2.9), writing it in a compact form

$$\mathbf{M} = \mathbf{V} - \int \mathbf{V}\, G\, \mathbf{M} \ , \tag{2.18}$$

where $\int = \int d^3\mathbf{k}$. Taking the Dirac conjugate of this equation yields

$$\overline{\mathbf{M}} = \mathbf{V} - \int \overline{\mathbf{M}}\, \overline{G}\, \mathbf{V}. \tag{2.19}$$

Following [11], we obtain

$$\overline{\mathbf{M}} - \mathbf{M} = -2i \int \overline{\mathbf{M}}\, \Delta G\, \mathbf{M}, \tag{2.20}$$

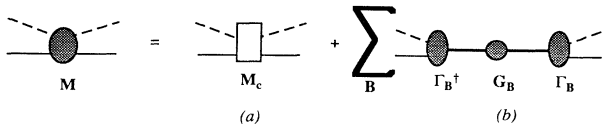

FIG. 22. Diagrammatic representation of the solution (2.12) to Eq. (2.9).

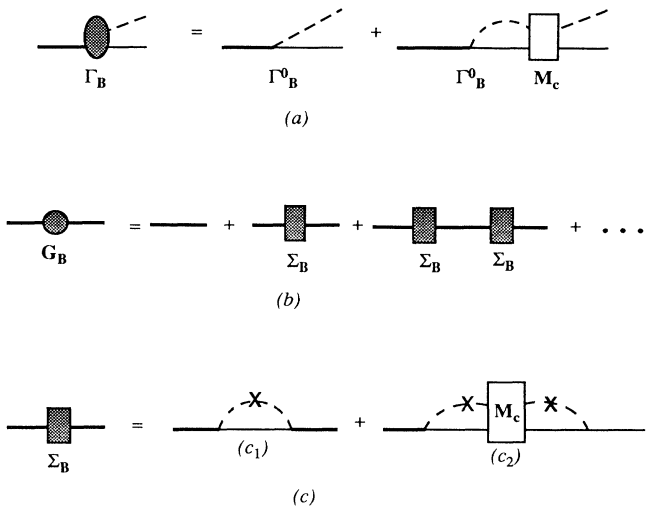

FIG. 23. Diagrammatic representation of (a) Eq. (2.14) for the dressed vertex function, (b) Eq. (2.15) for the dressed propagator, and (c) Eq. (2.16) for the self-energy.

where, in this case,

$$\Delta G = \pi\delta_+[m^2 - (P-k)^2]\left(\frac{m + \not{P} - \not{k}}{2\omega_k}\right). \tag{2.21}$$

Restoring the indicies and integrating over the magnitude of $\mathbf{k}$ gives, explicitly,

$$\overline{\mathbf{M}}_{\alpha'\alpha}(p',p,P) - \mathbf{M}_{\alpha'\alpha}(p',p,P)$$
$$= -i\frac{|\tilde{\mathbf{k}}|}{16\pi^2 W}\int d\Omega_{\tilde{k}}\overline{\mathbf{M}}_{\alpha'\alpha''}(p',\tilde{k},P) \times (m + \not{P} - \not{\tilde{k}})_{\alpha'',\alpha'''}\mathbf{M}_{\alpha'''\alpha}(\tilde{k},p,P), \tag{2.22}$$

where $\tilde{k} = (\omega_k, \tilde{\mathbf{k}})$ is the pion momentum when both nucleon and pion are on shell.

If we expand $(m + \not{P} - \not{\tilde{k}})_{\alpha\alpha'}$ in terms of Dirac spinors with helicity λ [38],

$$(m + \not{P} - \not{\tilde{k}})_{\alpha\alpha'} = 2m\sum_\lambda u_\alpha(\mathbf{p},\lambda)\ \bar{u}_{\alpha'}(\mathbf{p},\lambda), \tag{2.23}$$

and introduce

$$M^{++}_{\lambda'\lambda}(p',p,P) = \bar{u}_{\alpha'}(\mathbf{p}',\lambda')\mathbf{M}_{\alpha'\alpha}(p',p,P)u_\alpha(\mathbf{p},\lambda) \ , \tag{2.24}$$

we obtain

$$\overline{M}^{++}_{\lambda'\lambda}(p',p,P) - M^{++}_{\lambda'\lambda}(p',p,P)$$
$$= -i\frac{m|\tilde{\mathbf{k}}|}{8\pi^2 W}\sum_{\lambda''}\int d\Omega_{\tilde{k}}\ \overline{M}^{++}_{\lambda'\lambda''}(p',\tilde{k},P)M^{++}_{\lambda''\lambda}(\tilde{k},p,P). \tag{2.25}$$

Equation (2.25) is an exact statement of elastic unitarity.

III. MODEL

The results obtained in the previous section hold for any choice of the relativistic kernel (or potential). In this section, details of the model of pion nucleon scattering described in Sec. I are presented. The main goal is to calculate the scattering amplitudes shown diagrammatically in Fig. 22. The choice of form factors is discussed in Sec. III C, followed by a discussion of the treatment of each baryon resonance (N^*, Δ, and D_{13}) and the inelasticity.

A. Relativistic contact terms

The solution of the integral equation (2.13) is greatly simplified if the relativistic kernel V_c is approximated so that the two-pion production cut, which arises from the crossed pole driving terms, is eliminated. This approximation allows us to reduce the integral equation to a geometric series, which can be summed to give a closed form for the solution.

However, this approximation must be done very carefully, as these terms make important contributions to the S waves. We require that the approximation preserves chiral symmetry at threshold (which will give the correct scattering lengths), that it not depart significantly from the tree level calculation (where all external particles are on shell), and that it extrapolates smoothly to the nucleon pole. For the last requirement we extrapolate the amplitude off shell in the manner suggested by the structure of our integral equation; we constrain the pions to their mass shell and allow the nucleons to go off shell.

The exact crossed nucleon Born term with mixed coupling is

$$\begin{aligned}\mathbf{V}_c^N(p',p,P) = g^2\tau_i\tau_j &\left(\lambda\gamma^5 + \frac{(1-\lambda)}{2m}\not{k}\gamma^5\right)\\ &\times\frac{m+\not{P}-\not{k}-\not{k}'}{m^2-(W-k'-k)^2}\\ &\times\left(\lambda\gamma^5+\frac{(1-\lambda)}{2m}\gamma^5\not{k}'\right)\\ &\times f_N^2((p'-k)^2)f_N(p'^2)f_N(p^2)\end{aligned}\tag{3.1}$$

where τ_i and τ_j denote the isospin of nucleon coupled to the pion field i and j, and g is the bare πNN coupling. The nucleon form factor f_N will be described later in Sec. III C. This term can be written in the form

$$\begin{aligned}\mathbf{V}_c^N(p',p,P) = g^2\tau_i\tau_j\Bigg[&\left(a_1+b_1\frac{\not{Q}}{\mu}\right)+\frac{m-\not{p}'}{2m}\left(a_2+b_2\frac{\not{Q}}{\mu}\right)+\left(a_3+b_3\frac{\not{Q}}{\mu}\right)\frac{m-\not{p}}{2m}\\ &+\frac{m-\not{p}'}{2m}\left(a_4+b_4\frac{\not{Q}}{\mu}\right)\frac{m-\not{p}}{2m}\Bigg]f_N^2((p'-k)^2)f_N(p'^2)f_N(p^2),\end{aligned}\tag{3.2}$$

which displays its coupling, through the factors $m-\not{p}$ (or $m-\not{p}'$), to the negative energy sector. We will first assume that all the particles are on shell and neglect the off-diagonal part of $\not{Q}$ (which gives only a tiny contribution to the S waves). This gives us

$$\mathbf{V}_c^N(p',p,P) = Cg^2\tau_i\tau_j f_N(p'^2)f_N(p^2)f_N^2(u)\left(\frac{\lambda^2-1}{2m}+\left[\frac{1}{m^2-u}-\frac{(1-\lambda)^2}{4m^2}\right]\not{Q}\right) = \tilde{\mathbf{V}}_c^N(P)f_N(p'^2)f_N(p^2),\tag{3.3}$$

where C is a proportionality constant, $u=(p'-k)^2$, and

$$\not{Q} = \frac{W^2+\mu^2-m^2}{2W}\gamma^0.\tag{3.4}$$

Since we are interested in retaining the dominant S-wave terms only, we will also neglect the $\mathbf{p}'\cdot\mathbf{k}$ in u (this gives only a tiny contribution anyway). This gives

$$m^2-u = \frac{(W^2-m^2)(W^2+m^2-2\mu^2)-\mu^4}{2W^2}.\tag{3.5}$$

Finally, in order to obtain the correct limit at $W=m$, which is very important for a calculation of the stability condition, we have modified the second term of V_c as follows:

$$\begin{aligned}\frac{\not{Q}}{m^2-u} &= \frac{W(W^2+\mu^2-m^2)}{(W^2-m^2)(W^2+m^2-2\mu^2)-\mu^4}\gamma^0\\ &\sim\frac{W}{W^2+m^2-m\mu-2\mu^2}\gamma^0.\end{aligned}\tag{3.6}$$

This approximate expression is very close to the result we would have obtained if we had averaged the exact crossed diagram (evaluated below threshold by putting the pions on-shell) over the pion three-momentum (such as would occur when V_c is used as a kernel); it gives only a 6% error when used to evaluate the fourth order diagram. It is also very close to the exact tree diagram above threshold, as shown in Fig. 24. Note that the "tree approximation," the first form given in Eq. (3.6), gives a very bad result below threshold.

To restore the chiral symmetry which is broken by the pseudoscalar coupling, we introduce a σ-exchange term. A ρ-exchange term is also introduced in order get a good description of the S-wave scattering lengths. The σ and ρ exchanges are approximated as contact terms, and the ρ exchange is divided into two terms, one with a strength proportional to $(1-\lambda)^2$ and one independent of λ. The first of these, when combined with the σ-like exchange term, can be adjusted to give an interaction at the πN

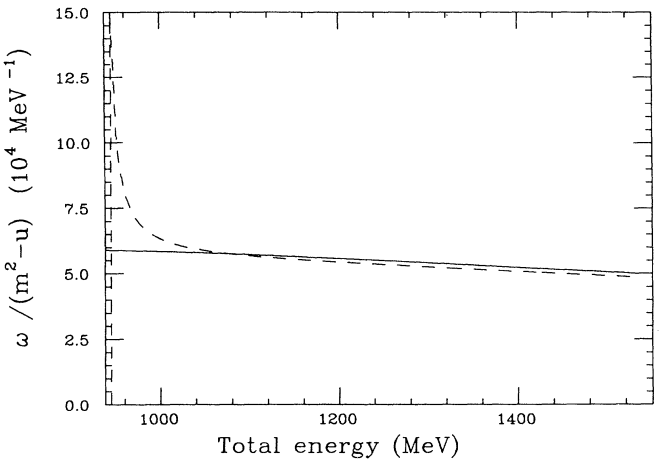

FIG. 24. Comparison of our approximation (solid line) with the exact tree result (dashed line). Both of these are defined in Eq. (3.6).

threshold which is independent of λ [recall Eq. (1.6)], while the second will have a strength which is independently adjustable [recall Eq. (1.10)]. Specifically, with the approximation for $\mathcal{Q}$ made above and with the form factors added, these two contact terms are

$$\tilde{\mathbf{V}}_c^{\sigma,\rho}(p',p,P) = -C\frac{g^2}{m}f_0^2\left[\delta_{ij}\lambda^2 + [\tau_j,\tau_i](1-\lambda)^2\frac{\mathcal{Q}}{4m}\right],$$
$$\tilde{\mathbf{V}}_c^{\rho}(p',p,P) = -C_\rho\frac{g^2}{4m^2}f_0^2[\tau_j,\tau_i]\mathcal{Q}, \tag{3.7}$$

where $\tilde{\mathbf{V}}_\mathbf{c}$ was defined in Eq. (3.3). Since it is very difficult to preserve chiral symmetry to all energies, we maintained it at threshold, which required the same form factors in all of the contact terms, and the condition

$$Cf_0^2 = f_N^2((m+\mu)^2) \ , \tag{3.8}$$

which determines the constant C.

The crossed diagrams for the baryon resonances (N^*, Δ, D_{13}) also were approximated in the same way as we approximated the nucleon crossed diagram, and in this approximation the Δ and D_{13} crossed diagrams are zero. The details of the treatment of the resonances will be discussed in Secs. III D–III F.

Finally, the total relativistic contact interaction

$$\mathbf{V}_c(p',p,P) = \mathbf{V}_c^N(p',p,P) + \mathbf{V}_c^{\sigma,\rho}(p',p,P) + \mathbf{V}_c^{\rho}(p',p,P) + \mathbf{V}_c^{N^*}(p',p,P) \tag{3.9}$$

can be written in the covariant form

$$\mathbf{V}_c(p',p,P) = \left(C_0(W)\frac{P}{W} + C_1(W)\right) f_N(p^2)f_N(p'^2). \tag{3.10}$$

B. Solving the integral equation for $\mathbf{M}_c$

In this section we would like to solve the integral equation (2.13) for the *background* amplitude $\mathbf{M}_c$. This equation is shown diagrammatically in Fig. 4(c), and is the first term in the full solution, as represented in Fig. 22(a). The driving terms for this equation are given in Eq. (3.10). The calculation of the dressed pole diagrams which complete the solution, as shown in Fig. 22(b), will be postponed until we discuss the resonances.

To calculate both background and the pole diagrams, it is more convenient if we use the projection operators

$$\Lambda^\pm = \frac{1 \pm \gamma^0}{2}. \tag{3.11}$$

In terms of these projection operators, Eq. (3.10) becomes

$$\mathbf{V}_c(p',p,P) = (V_c^+\Lambda^+ + V_c^-\Lambda^-)f_N(p^2)f_N(p'^2) \ , \tag{3.12}$$

where

$$V_c^\pm = C_1(W) \pm C_0(W). \tag{3.13}$$

Since $V_c^\pm$ only depends on the total momentum $P = (W,\mathbf{0})$, the integral equation (2.13) is a geometric series, which can be summed in closed form. The result is

$$M_c(p',p,P) = (M_c^+\Lambda^+ + M_c^-\Lambda^-)f_N(p^2)f_N(p'^2) \ , \tag{3.14}$$

where

$$M_c^\pm = \frac{V_c^\pm}{1 + V_c^\pm(mI_0 \pm WI_0 \mp \mu I_1)} \ . \tag{3.15}$$

The integrals I_n, which arise from the bubble integrations shown in Fig. 4(c), are

$$I_n = \int \frac{d^3\mathbf{k}}{(2\pi)^3}\left(\frac{\omega_k}{\mu}\right)^n \frac{f_N^2((P-k)^2)}{2\omega_k\,(m^2-(P-k)^2-i\epsilon)}. \tag{3.16}$$

C. Form factors

Form factors are needed to ensure that the integrals in Eqs. (2.13), (2.14), and (2.16) converge. Ideally, the results should be insensitive to the details of the form factors.

The form factors for the nucleon and N^* have the form

$$f_B(p^2) = \left(\frac{(\Lambda_B^2 - m_B^2)^2}{(\Lambda_B^2 - m_B^2)^2 + (m_B^2 - p^2)^2}\right)^2 \ , \tag{3.17}$$

where Λ_B is the form factor cuttoff mass, and m_B is the dressed baryon mass (recall, as we discussed above, that the dressed nucleon mass is equal to the bare nucleon mass). Ideally, the same form should be used for the Δ and Δ', the delta which appears inside the $\pi\Delta'$ loops which generate the inelasticities of the N^* and D_{13} resonances, but we found that the same form (3.17) did not work unless we replaced m_B by m, the nucleon mass. The behavior of these factors for various illustrative cases has already been shown in Figs. 16 and 17.

The form factor (3.17) not only gives $f_B(m_B^2) = 1$,

but also satisfies the criteria that was suggested for the form factor in Ref. [11]. The form factor should be only a function of p^2, decrease at most like a power of p^2 as $p^2 \to \infty$, and have no pole on the real axis.

D. Treatment of the coupled NN^* system

In this section we will first calculate the contribution of the N^* to the background diagram [Fig. 22(a)] and then calculate the N^* pole contributions. Since N^* has the same properties as the nucleon, we treat it like a heavy nucleon. The Feynman rule for the $N^*N\pi$ vertex is

$$g_{N^*}\left(\lambda^* + \frac{(1-\lambda^*)\not{k}}{m+m^*}\right)\gamma^5, \tag{3.18}$$

where g_{N^*} is the πNN^* coupling constant, m^* is the N^* mass, and λ^* is the mixing parameter for the πNN^* coupling. The reduced (with the external nucleon form factors removed) N^* crossed diagram can be written

$$\begin{aligned}\tilde{\mathbf{V}}_c^{N^*} &= g_{N^*}^2\left(\lambda^* + \frac{(1-\lambda^*)\not{k}}{m+m^*}\right)\gamma^5\left(\frac{m^*+\not{p}'-\not{k}}{m^{*2}-(p'-k)^2}\right)\gamma^5\left(\lambda^* + \frac{(1-\lambda^*)\not{k}'}{m+m^*}\right)\tau_i\tau_j \\ &\simeq g_{N^*}^2\left[\frac{m^*-m}{m^{*2}-u} + \frac{\lambda^{*2}-1}{m+m^*} + \not{Q}\left(\frac{1}{m^{*2}-u} - \frac{(1-\lambda^*)^2}{(m+m^*)^2}\right)\right]\tau_i\tau_j,\end{aligned} \tag{3.19}$$

where u is approximated as before. We chose $\lambda^* = 1$.

To calculate the dressed pole terms [Fig. 22(b)] coming from the coupled NN^* system, we first calculate the dressed propagators for the N and N^*, including the transition from N^* to N and vice versa. This requires that we diagonalize the inverse propagator matrix

$$G^{-1} = \begin{pmatrix} g_{11} & g_{12} \\ g_{21} & g_{22} \end{pmatrix} = \begin{pmatrix} m - \not{P} + \Sigma_{11} & \Sigma_{12} \\ \Sigma_{21} & m^* - \not{P} + \Sigma_{22} \end{pmatrix}, \tag{3.20}$$

where Σ_{ij} is the self-energy, and the indicies i, j can be either 1 (for nucleons) or 2 (for N^*). Note that this matrix is symmetric, but not Hermitian. It can be diagonalized by a complex symmetric matrix

$$G_d^{-1} = A\,G^{-1}\,A, \tag{3.21}$$

where, choosing the simple form for A,

$$A = \begin{pmatrix} 1 & Z \\ Z & 1 \end{pmatrix}, \tag{3.22}$$

gives the following results for the diagonal elements of G_d:

$$\begin{aligned} G_{11} &= \frac{1}{(m - \not{P} + \Sigma_{11}) + (2\Sigma_{12})Z + (m^* - \not{P} + \Sigma_{22})Z^2}, \\ G_{22} &= \frac{1}{(m^* - \not{P} + \Sigma_{22}) + (2\Sigma_{12})Z + (m - \not{P} + \Sigma_{11})Z^2}, \end{aligned} \tag{3.23}$$

where

$$Z = \frac{-(g_{11}+g_{22}) \pm \sqrt{(g_{11}+g_{22})^2 - 4g_{12}^2}}{2g_{12}}. \tag{3.24}$$

It turns out that the quantity $g_{11} + g_{22}$ is negative, and hence we must choose the minus sign in (3.24) in order that $Z \to 0$ as $g_{12} \to 0$.

The contributions of these terms to the scattering matrix M is

$$\begin{aligned} M &= \Gamma^\dagger G \Gamma = \Gamma^\dagger (G^{-1})^{-1}\Gamma \\ &= \Gamma^\dagger (A^{-1}AG^{-1}AA^{-1})^{-1}\Gamma = \Gamma^\dagger (A^{-1}G_d^{-1}A^{-1})^{-1}\Gamma \\ &= \Gamma^\dagger A G_d A \Gamma\,, \end{aligned} \tag{3.25}$$

where the unmixed vertex column vector Γ is

$$\Gamma = \begin{pmatrix} \Gamma_{\pi NN} \\ \Gamma_{\pi NN^*} \end{pmatrix}. \tag{3.26}$$

The *dressed* vertices are therefore

$$\begin{aligned} \Gamma_{\pi NN}^{\text{dressed}} &= \Gamma_{\pi NN} + Z\Gamma_{\pi NN^*}, \\ \Gamma_{\pi NN^*}^{\text{dressed}} &= \Gamma_{\pi NN^*} + Z\Gamma_{\pi NN}. \end{aligned} \tag{3.27}$$

The mixing therefore depends on Z, which is dependent on energy and is complex above the pion production threshold. The values of Z at the nucleon mass and the dressed Roper mass are given in Table I; note that Z is very small. Note that this treatment extends that of Pearce and Afnan [39], which can be applied only below the πN threshold where all the matrix elements are real.

Each of these propagators and the corresponding dressed vertex functions can be written in terms of the projection operators $\Lambda_\pm$ of Eq. (3.11), and then the contributions from the dressed N and N^* pole terms to the scattering matrix, part of the sum shown in Fig. 22(b), can be easily expressed in this form as well:

$$M = M_+\Lambda_+ + M_-\Lambda_-\,. \tag{3.28}$$

These two poles contribute to spin $\frac{1}{2}$ (S and P) partial wave amplitudes.

E. Treatment of the Δ

In this section we review the properties of the spin 3/2 propagator which we have used in this calculation, and calculate the contribution of the dressed Δ pole to the scattering amplitude [Fig. 22(b)].

We start with the most general form of the spin 3/2 propagator:

$$\Delta_{\mu\nu}(P) = \frac{-i(m_\Delta + \not{P})}{(m_\Delta^2 - P^2 - i\epsilon)}\theta_{\mu\nu}(P), \tag{3.29}$$

where

$$\theta_{\mu\nu}(P) = ag_{\mu\nu} + b\gamma_\mu\gamma_\nu + c\frac{\not{P}\gamma_\mu P_\nu}{P^2} + d\frac{P_\mu\gamma_\nu\not{P}}{P^2}, \tag{3.30}$$

where P is the four-momenta of the Δ and m_Δ is its mass.

To get a pure spin 3/2 propagator, we impose two conditions which eliminate the virtual spin 1/2 and spin 1 parts:

$$\gamma^\mu\theta_{\mu\nu}(P) = 0, \tag{3.31}$$

$$P^\mu\theta_{\mu\nu}(P) = 0 \ . \tag{3.32}$$

From these two conditions we get

$$b = c = d = \frac{1}{3}a. \tag{3.33}$$

Choosing $a = -1$ gives

$$\theta_{\mu\nu}(P) = -g_{\mu\nu} + \frac{1}{3}\gamma_\mu\gamma_\nu + \frac{1}{3}\left(\frac{\not{P}\gamma_\mu P_\nu + P_\mu\gamma_\nu\not{P}}{P^2}\right). \tag{3.34}$$

We will exploit several properties of $\theta_{\mu\nu}(P)$. In addition to Eq. (3.32), we will use

$$\not{P}\theta_{\mu\nu}(P) = \theta_{\mu\nu}(P)\not{P},$$

$$\theta_\mu{}^\beta(P)\theta_{\beta\nu}(P) = -\theta_{\mu\nu}(P) \ . \tag{3.35}$$

To calculate the self energy of the Δ, we need the Feynman rule for the coupling of the Δ with pion-nucleon channel. For this coupling we take

$$\Gamma^0_{\Delta\,\alpha}(P,p') = \left(\frac{g_\Delta}{\mu}\right) f_\Delta(P^2)[\theta_{\mu\nu}(P)]_{\beta\alpha}k^\nu f_N(p'^2)T_i, \tag{3.36}$$

where g_Δ is the bare $\pi N\Delta$ coupling, T_i is the isospin $3/2 \to 1/2$ transition operator for an incoming pion with isospin i, $f_N(p'^2)$ is the nucleon form factor, $f_\Delta(P^2)$ is the delta form factor, k is the momentum of the incoming pion, and α is the Dirac index of the incoming nucleon. (The Dirac index β and Lorentz index μ of the outgoing Δ are suppressed in Γ.) Note that T_i is related to τ_i by the relation [40]

$$T_j^\dagger T_i = 2(\delta_{ji} - \tfrac{1}{3}\tau_j\tau_i). \tag{3.37}$$

The Δ self-energy [only the first term of Fig. 23(c) contributes because the second term does not couple to the P_{33} channel] can be written

$$\Sigma^{\mu\nu}(P) = \left(\frac{g_\Delta}{\mu}\right)^2 \frac{2}{(2\pi)^3} f_\Delta^2(P^2) \times \int \frac{d^3\mathbf{k}}{2\omega_k} \frac{f_N^2((P-k)^2)}{m^2 - (P-k)^2 - i\epsilon} \times \theta^{\mu\alpha}(P)k_\alpha(m + \not{P} - \not{k})(-k_\beta)\theta^{\beta\nu}(P). \tag{3.38}$$

The angular integration can be carried out using the formulae given in Appendix B. Using the properties of $\theta^{\mu\nu}(P)$, the dressed propagator becomes

$$G^{\mu\nu}_\Delta(P) = \frac{-i\,\theta^{\mu\nu}(P)}{m_\Delta - \not{P} + \Sigma_\Delta(P)} \ . \tag{3.39}$$

The dressed vertex is calculated from Fig. 23(a). However, only the first term (the bare vertex) will contribute; the second term is zero [using the properties of $\theta^{\mu\nu}(P)$ after doing the angular integration]. Then the contribution of the dressed Δ pole to the scattering matrix is

$$M_\Delta = -\left(\frac{g_\Delta}{\mu}\right)^2 f_\Delta^2(P^2)\,T_jT_i \times \frac{k'^\alpha\theta_{\alpha\mu}(P)\,\theta^{\mu\nu}(P)\,\theta_{\nu\beta}(P)k^\beta}{m_\Delta - \not{P} + \Sigma_\Delta(P)}T_i\,, \tag{3.40}$$

which can be reduced using the properties of the $\theta_{\mu\nu}(P)$.

F. Treatment of the D_{13}

In this section we calculate the scattering amplitude for the D_{13} dressed pole term. The calculation of this pole term is similar to the Δ pole term just calculated, except there is an extra γ^5 in the πND_{13} coupling. We write the interaction Lagrangian for the πND_{13} coupling as

$$L = \left(\frac{g_D}{\mu}\right)\bar\Psi^\mu_{D_{13}}\theta_{\mu\nu}\,\tau_i\,\gamma^5\Psi_N\,\frac{\partial\phi^i}{\partial x_\nu} + \text{H.c.}, \tag{3.41}$$

where g_D is the coupling constant and $\theta_{\mu\nu}$ is the spin 3/2 projection operator which is described in the previous section. From this Lagrangian one can derive a Feynman rule for the πND_{13} interaction vertex

$$\Gamma^0_{D\,\alpha}(P,p') = i\left(\frac{g_D}{\mu}\right)[\theta_{\mu\nu}(P)]_{\beta\alpha}k^\nu\gamma^5 f_N(p'^2)\,\tau_i \ . \tag{3.42}$$

Note that no form factor for the D_{13} is used. Using this coupling, D_{13} propagator becomes

$$G^{\mu\nu}_D(P) = \frac{-i\,\theta^{\mu\nu}(P)}{m_D - \not{P} + \Sigma_D(P)}, \tag{3.43}$$

where $\Sigma_D(P)$ is the self-energy of the D_{13} and m_D is its bare mass. As in the case of the Δ, the self-energy of the D_{13} is given completely by the first term in Fig. 23(c),

$$\Sigma^{\mu\nu}_D(P) = \left(\frac{g_D}{\mu}\right)^2 \frac{\tau_i\tau_i}{(2\pi)^3} \times \int \frac{d^3\mathbf{k}}{2\omega_k} \frac{f_N^2((P-k)^2)}{m^2 - (P-k)^2 - i\epsilon} \times\theta^{\mu\alpha}(P)k_\alpha\gamma^5(m + \not{P} - \not{k})\gamma^5 k_\beta\theta^{\beta\nu}(P). \tag{3.44}$$

The scattering amplitude is calculated in the same way as the Δ channel. The D_{13} resonance contributes only to the D_{13} and P_{13} partial waves.

G. Inelastic channels

It is well known that the inelastic channels become more and more important as we go to higher and higher energy. In this analysis we consider the inelasticity from the P_{11} and D_{13} channels which is dominated by π-Δ scattering. We approximate the finite width Δ by a zero width Δ', which has the same properties as Δ except of its mass.

Now calculate the inelasticity of the P_{11} channel. Figure 25(a) can be written

$$\Sigma = \left(\frac{g'_{N^*}}{\mu}\right)^2 f^2_{N^*}(P)\frac{2}{(2\pi)^3} \times \int \frac{d^3\mathbf{k}}{2\omega_k}\frac{f^2_{\Delta'}((P-k)^2)}{m^2_{\Delta'}-(P-k)^2-i\epsilon} \times k^\mu \theta_{\mu\alpha}(P-k)(m_{\Delta'}+\not{P}-\not{k}) \times \theta^{\alpha\beta}(P-k)\theta_{\beta\nu}(P-k)(-k^\nu). \quad (3.45)$$

Since $(\not{P}-\not{k})$ commutes with $\theta_{\mu\alpha}(P-k)$, the tensor calculation can be carried out easily, and the angle integration can be carried out using the formulas in Appendix B.

For the D_{13} inelasticity, we start from a Feynman rule for an interaction between D_{13}, Δ', and π,

$$\Gamma^{o'}_D(p,p') = i\, g'_D \theta_{\mu\alpha}(p)\theta^{\alpha\nu}(p')f_{\Delta'}(p'^2)T_i \quad , \quad (3.46)$$

where p and p' are the momentum of the D_{13} and Δ' respectively and T_i is the isospin 3/2 to 1/2 transition operator. The self-energy for this channel [Fig. 25(b)] can be written

$$\Sigma_{\mu\nu}(P) = -(g'_D)^2\frac{2}{(2\pi)^3}\theta_{\mu\alpha}(P) \times \int \frac{d^3\mathbf{k}}{2\omega_k}\frac{f^2_{\Delta'}((P-k)^2)}{m^2_{\Delta'}-(P-k)^2-i\epsilon} \times \theta^{\alpha\epsilon}(P-k)(m_{\Delta'}+\not{P}-\not{k}) \times \theta_{\epsilon\gamma}(P-k)\theta^{\gamma\delta}(P-k)\theta_{\delta\nu}(P). \quad (3.47)$$

This equation can be simplified using the properties of $\theta_{\mu\nu}(P)$ and the angular integrations given in Appendix B. Details of these calculation can be found in [41].

ACKNOWLEDGMENTS

It is a pleasure to acknowledge helpful conversations with Simon Capstick, B. K. Jennings, and Nimai Mukhopadhyay. This work was supported by the DOE under Grant No. DE-FG05-88ER40435.

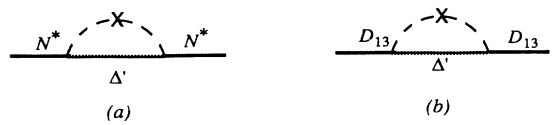

FIG. 25. Diagrams for estimating the inelasticities of the N^* and the D_{13}.

APPENDIX A: ALTERNATIVE FORMS FOR THE INTEGRAL EQUATION

First, we show that

$$\Gamma(p',P) = \Gamma_0(p',P) + \int d^3\mathbf{k}\; V_c(p',k,P)G_0(k,P)\Gamma(k,P) \quad (A1)$$

is equivalent to

$$\Gamma(p',P) = \Gamma_0(p',P) + \int d^3\mathbf{k}\; M_c(p',k,P)G_0(k,P)\Gamma_0(k,P), \quad (A2)$$

where Γ_0 is the bare vertex, Γ is the dressed vertex, M_c is the scattering matrix with the crossed diagrams as driving terms, and V_c stands for the potential (crossed diagrams). In this appendix we absorb the minus sign in front of the integral in Eq. (2.9) into G_0, giving a plus sign in Eq. (A1).

To carry out the proof, simplify the notation, and use the scattering equation

$$M_c = V_c + V_c G_0 M_c \quad (A3)$$

to write the *second term* in Eq. (A1) in the form

$$V_c G_0 \Gamma = M_c G_0 \Gamma - V_c G_0 M_c G_0 \Gamma. \quad (A4)$$

Now since

$$V_c G_0 M_c = M_c G_0 V_c, \quad (A5)$$

Eq. (A4) becomes

$$V_c G_0 \Gamma = M_c G_0 \Gamma - M_c G_0 V_c G_0 \Gamma. \quad (A6)$$

Substituting Eq. (A1) into (A6) gives

$$V_c G_0 \Gamma = M_c G_0 \Gamma - M_c G_0(\Gamma - \Gamma_0) = M_c G_0 \Gamma_0 \quad (A7)$$

Finally substituting Eq. (A7) into Eq. (A1) gives Eq. (A2), in the shorthand notation

$$\Gamma = \Gamma_0 + M_c G_0 \Gamma_0. \quad (A8)$$

Next, prove that

$$M = M_c + \Gamma G \Gamma^\dagger \quad (A9)$$

is equal to the infinite sum of all the possible diagrams generated from driving terms which are the sum direct and contact diagrams,

$$M = (V_c + V_d) + (V_c + V_d)G_0 M. \quad (A10)$$

Here M is the scattering matrix, V_d is the direct potential, G_0 is the *two-body* propagator, and $\tilde{G}_0$ and G are the bare and dressed propagator of the baryon, where

$$G = \tilde{G}_0 + \tilde{G}_0\, \Gamma_0^\dagger G_0 \Gamma\, G \quad . \quad (A11)$$

Proof:

$$\begin{aligned} V_cG_0M &= V_cG_0M_c + V_cG_0\Gamma G\Gamma^\dagger \\ &= M_c - V_c + V_cG_0\Gamma G\Gamma^\dagger \\ &= M_c - V_c + \Gamma G\Gamma^\dagger - \Gamma_0 G\Gamma^\dagger \\ &= M - V_c - \Gamma_0 G\Gamma^\dagger, \end{aligned} \tag{A12}$$

where we used Eqs. (A9), (A3), and (A1).

Now consider the direct term, which in this notation is $V_d = \Gamma_0\tilde{G}_0\Gamma_0^\dagger$. Hence

$$\begin{aligned} V_dG_0M &= \Gamma_0\tilde{G}_0\Gamma_0^\dagger G_0(M_c + \Gamma G\Gamma^\dagger) \\ &= \Gamma_0\tilde{G}_0(\Gamma^\dagger - \Gamma_0^\dagger) + \Gamma_0(G - \tilde{G}_0)\Gamma^\dagger \\ &= \Gamma_0 G\Gamma^\dagger - \Gamma_0 G_0\Gamma_0^\dagger, \end{aligned} \tag{A13}$$

where we used the complex conjugate of Eqs. (A8) and (A11).

Adding Eq. (A12) to Eq. (A13) yields

$$\begin{aligned} (V_c + V_d)G_0M &= M - V_c - \Gamma_0 G_0\Gamma_0^\dagger \\ &= M - V_c - V_d, \end{aligned} \tag{A14}$$

which is the same as Eq. (A10).

APPENDIX B: ANGULAR INTEGRALS

$$\int \not{k} d\Omega_k = \frac{4\pi \not{P}}{W}\omega_k, \tag{B1}$$

$$\int k^\mu d\Omega_k = \frac{4\pi P^\mu}{W}\omega_k, \tag{B2}$$

$$\int k^\mu \not{k} d\Omega_k = 4\pi\frac{P^\mu \not{P}}{W^2}\left(\omega_k^2 + \frac{1}{3}\mathbf{k}^2\right) - 4\pi\gamma^\mu\frac{1}{3}\mathbf{k}^2, \tag{B3}$$

$$\int k^\mu k^\nu d\Omega_k = 4\pi\frac{P^\mu P^\nu}{W^2}\left(\omega_k^2 + \frac{1}{3}\mathbf{k}^2\right) - 4\pi g^{\mu\nu}\frac{1}{3}\mathbf{k}^2, \tag{B4}$$

$$\begin{aligned} \int k^\mu k^\nu \not{k} d\Omega_k &= 4\pi\frac{P^\mu P^\nu \not{P}}{W^3}\omega_k\left(\omega_k^2 + \mathbf{k}^2\right) \\ &\quad -4\pi g^{\mu\nu}\frac{1}{3}\mathbf{k}^2\frac{\not{P}}{W}\omega_k \\ &\quad -\left(\frac{4\pi}{3}\mathbf{k}^2\omega_k\right)\frac{\gamma^\mu P^\nu + P^\mu\gamma^\nu}{W}. \end{aligned} \tag{B5}$$

APPENDIX C: PHASE SHIFTS AND CROSS SECTION

The phase shift is calculated using

$$-\frac{M_{l\pm}}{a} = \frac{\eta_{l\pm}e^{2i\delta_{l\pm}} - 1}{2i}, \tag{C1}$$

where $\eta_{l\pm}$ and $\delta_{l\pm}$ are the inelasticity parameter and phase shift. The $\pm$ refers to $j = l \pm \frac{1}{2}$ and a is defined by

$$a = \frac{8\pi^2 W}{m|\tilde{\mathbf{k}}|}, \tag{C2}$$

where $\tilde{\mathbf{k}}$ is the on-shell momentum in the c.m. system. The inelasticity parameter $\eta_{l\pm}$ can be calculated from

$$\frac{\eta_{l\pm}^2}{4} = \Re\left(\left|\frac{M^{l\pm}}{a}\right|\right)^2 + \left[\frac{1}{2} + \Im\left(\frac{M^{l\pm}}{a}\right)\right]^2. \tag{C3}$$

This formula can be obtained easily from Eq. (C1). The total crossed section formula is

$$\sigma_{\rm tot}^I = \frac{4\pi}{\tilde{\mathbf{k}}}\sum_{l=0}^{\infty}[(l+1)\Im(f_{l+}) + l\Im(f_{l-})], \tag{C4}$$

where

$$f_{l\pm} = -\frac{M_{l\pm}}{a}. \tag{C5}$$

For the π^+P system,

$$\sigma_{\rm tot} = \sigma_{\rm tot}^{I=3/2}, \tag{C6}$$

and for π^-P system, we have

$$\sigma_{\rm tot} = \tfrac{1}{3}(\sigma_{\rm tot}^{I=3/2} + 2\sigma_{\rm tot}^{I=1/2}). \tag{C7}$$

APPENDIX D: WIDTH, EFFECTIVE MASS AND EFFECTIVE COUPLING

To calculate the width, the effective mass of resonances, and effective coupling constant of resonance particles, we start from the pole diagrams in the scattering amplitudes (for the D_{13} and Δ we have only 1 diagram, but for P_{11} channel, after diagonalization, we have two pole diagrams as discussed in Sec. III).

These scattering amplitudes can be written in the form

$$M(W) = \frac{g_B^2 f(W)}{m^* - W - i\Gamma/2}, \tag{D1}$$

where g_B is the pion-baryon coupling constant. The imaginary part of this $M(W)$ (at $W = m^*$) is

$$\Im(M(m^*)) = \frac{g_B^2 f(m^*)}{\Gamma/2}. \tag{D2}$$

Taking the real part of the derivative of Eq. (D1) gives

$$\Re\left(\frac{\partial M(m^*)}{\partial W}\right) = -\frac{g_B^2 f(m^*)}{\Gamma^2/4}, \tag{D3}$$

and from Eqs. (D2) and (D3),

$$\Gamma = -\frac{2\Im M(m^*)}{\Re\frac{\partial M(m^*)}{\partial W}}. \tag{D4}$$

The effective mass m^* is calculated using Eq. (1.12).

The effective pion-baryon coupling constant can also be derived from Eq. (D2),

$$g_B^2 = \frac{\Gamma\Im M(m^*)}{2f(m^*)}. \tag{D5}$$

[1] G. F. Chew and F. E. Low, Phys. Rev. **101**, 1570 (1956).
[2] S. D. Drell, M. H. Freedman, and F. Zachariasen, Phys. Rev. **104**, 236 (1956).
[3] S. Weinberg, Phys. Rev. Lett. **17**, 616 (1966).
[4] H. Schnitzer, Phys. Rev. **158**, 1471 (1967).
[5] S. Weinberg, Phys. Rev. Lett. **18**, 188 (1967).
[6] R. D. Peccei, Phys. Rev. **176**, 1812 (1968).
[7] B. Dutta-Roy, I. R. Lapidus, and M. J. Tausner, Phys. Rev. **181**, 2091 (1969); **177**, 2529 (1969).
[8] M. K. Banerjee and J. B. Cammarata, Phys. Rev. D **16**, 1977 (1334).
[9] B. C. Pearce and B. K. Jennings, Nucl. Phys. **A528**, 655 (1991).
[10] F. L. Gross, J. W. Van Orden, and K. Holinde, Phys. Rev. C **41**, R1909 (1990).
[11] F. L. Gross, J. W. Van Orden, and K. Holinde, Phys. Rev. C **45**, 2094 (1992).
[12] R. E. Behrends and C. Fronsdal, Phys. Rev. **106**, 345 (1957).
[13] H. T. Williams, Phys. Rev. C **31**, 2297 (1985).
[14] M. Benmerrouche, R. M. Davidson, and N. C. Mukhopadhyay, Phys. Rev. C **39**, 2339 (1989).
[15] T. Mizutani *et al.*, Phys. Rev. C **24**, 2633 (1981).
[16] S. Morioka and I. R. Afnan, Phys. Rev. C **26**, 1148 (1981).
[17] E. Oset, H. Toki, and W. Weise, Phys. Rep. **83**, 282 (1982).
[18] Particle Data Group, K. Hikasa *et al.*, Phys. Rev. D **45**, S1 (1992).
[19] J. Frohlich, K. Schwarz, L. Streit, and H. F. K. Zingl, Phys. Rev. C **25**, 2591 (1982).
[20] K. Schwarz, H. F. K. Zingl, and L. Mathelitsch, Phys. Lett. **83B**, 297 (1979).
[21] R. M. Woloshyn and A. D. Jackson, Nucl. Phys. **B64**, 269 (1973), and references therein.
[22] E. D. Cooper and B. K. Jennings, Nucl. Phys. **A483**, 601 (1988).
[23] F. L. Gross, Phys. Rev. **186**, 1448 (1969).
[24] F. L. Gross, Phys. Rev. C **26**, 2203 (1982).
[25] G. F. Chew, Phys. Rev. **95**, 1669 (1954).
[26] K. Nishijima, *Fields and Particles* (Benjamin, New York, 1969).
[27] M. Gell-Mann and M. Levy, Nuovo Cimento **16**, 705 (1960).
[28] J. Wess and B. Zumino, Phys. Rev. **163**, 163 (1967); Y. Tomozawa and Y. P. Yao, Phys. Rev. Lett. **18**, 1084 (1967); P. Chang and F. Gursey, Phys. Rev. **164**, 1752 (1967).
[29] F. L. Gross, K. M. Maung, J. A. Tjon, L. W. Townsend, and S. J. Wallace, Phys. Rev. C **40**, R10 (1989); K. M. Maung, F. L. Gross, J. A. Tjon, L. W. Townsend, and S. J. Wallace, *ibid.* **43**, 1378 (1991).
[30] P. F. A. Goudsmit, H. J. Leisi, and E. Matsinos, Report No. ETHZ-IMP PR/91-6, 1991.
[31] R. Arndt and S. Roper, Scattering Analysis and Interactive Dial-in (SAID) program, Virginia Polytechnic Institute and State University, 1991.
[32] R. Koch *et al.*, Nucl. Phys. **A336**, 331 (1980).
[33] E. Bovet, Phys. Lett. **153B**, 231 (1985).
[34] M. Fierz and W. Pauli, Proc. R. Soc. London A **173**, 211 (1939).
[35] W. Rarita and J. Schwinger, Phys. Rev. **60**, 61 (1941).
[36] W. Jaus and W. S. Woolcock, Nuovo Cimento A **97**, 103 (1987).
[37] F. L. Gross and D. O. Riska, Phys. Rev. C **36**, 1928 (1987).
[38] M. Jacob and G. C. Wick, Ann. Phys. (N.Y.) **7**, 404 (1959).
[39] B. Pearce and I. R. Afnan, Phys. Rev. C **40**, 220 (1989).
[40] T. Ericson and W. Weise, *Pions and Nuclei* (Oxford University Press, New York, 1988).
[41] Ph.D. thesis (part I), Yohanes Surya, 1993 (unpublished).